# MASTERARBEIT | MASTER'S THESIS

Titel | Title

New insights into the locomotion and feeding of the epaulette shark, Hemiscyllium ocellatum (Bonnaterre, 1788) (Elasmobranchii, Orectolobiformes)

verfasst von | submitted by

Rafael-Claus Pichler, BSc.

angestrebter akademischer Grad | in partial fulfilment of the requirements for the degree of

Master of Science (MSc)

Wien | Vienna, 2025

| | |
|---|---|
| Studienkennzahl lt. Studienblatt \| Degree programme code as it appears on the student record sheet: | UA 066 831 |
| Studienrichtung lt. Studienblatt \| Degree programme as it appears on the student record sheet: | Masterstudium Zoologie |
| Betreut von \| Supervisor: | Univ.-Prof. Dipl.-Geol. Dr. Jürgen Kriwet |

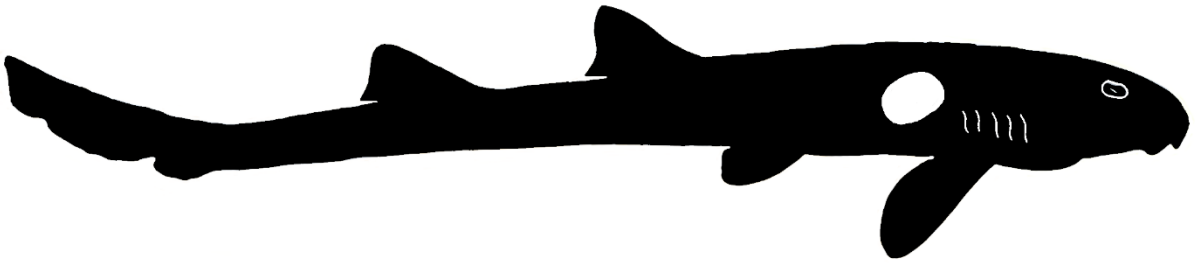

# Table of Contents

## Abstract

Sharks inhabit a wide variety of aquatic habitats around the globe. This great diversity of environments leads to a multitude of adaptations to accommodate them. The most striking are body shape, type of locomotion and feeding strategies. *Hemiscyllium ocellatum*, the epaulette shark, a bottom dwelling suction feeder, is known for hunting in tidal pools and coral reefs from Northern Australia to Southern New Guinea. In order to thrive in such conditions, it is necessary to possess both an extraordinary mode of locomotion and an innate resistance to the prevailing circumstances. Resisting the low oxygen concentration and high temperature, the epaulette shark walks on top of coral reefs, using his paired fins, to reach its hunting grounds. Once there he captures prey through powerful suction. *Hemiscyllium ocellatum* has already been the subject of numerous studies taking a closer look at its resistances and morphology. Also, three modes of locomotion were discovered: swimming, a slow walking trot and a fast walking trot. Nevertheless, this study has gained new insights into the morphological and morphofunctional properties of the “walking shark”. Using a combination of dissection, micro-CT imaging and in vivo video observations, a morphological overview as well as new locomotion patterns were described for this species. From a morphological point of view, this study aims to determine the specific muscles, muscle groups and components of the cartilaginous skeleton that are responsible for the unique locomotion for which *Hemiscyllium ocellatum* is renowned. New insights were gained about the *muscules inclinatores dorsales*, a muscle complex enabling specific motor skills of the dorsal fins, whose structure has recently been redescribed and compared between different shark genera and families. As the aforementioned study did not include *Hemiscyllium ocellatum*, this species was examined in greater detail, according to the hypothesis that these muscle systems play pivotal roles in the contralateral dorsal fin movement observed in videographic recordings. The video analysis presents a step-by-step description of the epaulette sharks walking trot and a newly described motion pattern which was found during suction feeding. This work constitutes the basis for further studies in the fields of comparative morphology and detailed descriptions of locomotion patterns across all shark families.

## Zusammenfassung

Haie besiedeln eine bemerkenswerte Bandbreite aquatischer Lebensräume rund um den Globus. Diese ökologische Vielfalt hat im Laufe der Evolution zu einer großen Diversität an Anpassungen geführt. Am auffälligsten sind dabei Unterschiede in Körperform, Fortbewegungsstrategien und Ernährungstypen. *Hemiscyllium ocellatum*, der Epaulettenhai, eine bodenlebende Art, ist in Gezeitentümpeln und Korallenriffen von Nordaustralien bis Süd-Neuguinea heimisch. Um in diesen teils extremen Umweltbedingungen zu überleben, bedarf es sowohl einer außergewöhnlichen Fortbewegungsweise als auch angeborener Resistenzen. Mit Hilfe seiner paarigen Brust- und Bauchflossen, ist es dem Epaulettenhai möglichsich laufähnlich fortzubewegen. Somit kann er gezielt über Korallenstrukturen und felsigen Untergrund zu bevorzugten Jagdarealen gelangen, wo er seine ausgeprägte Saugkraft nutzt, um Beutetiere effizient zu erfassen. *Hemiscyllium ocellatum* wurde bereits mehrfach hinsichtlich seiner Resilienz und anatomischen Besonderheiten untersucht. Unter anderem konnten dabei drei distinkte Fortbewegungsmodi identifiziert werden: Schwimmen, langsames Gehen und schnelles Gehen. Diese Arbeit liefert neue Erkenntnisse zur Morphologie und funktionellen Anatomie. Durch Kombination von Präparationstechniken, Mikro-CT-Bildgebung und in-vivo-Videoanalysen konnte sowohl ein morphologischer Überblick als auch bislang nicht beschriebene Bewegungsmuster dokumentiert werden. Der Fokus lag dabei auf muskulären und knorpeligen Strukturen, welche die Basis für die außergewöhnliche Fortbewegung bilden, wie die *Musculi inclinatores dorsales*, ein Muskelkomplex, welcher spezifische Bewegungen der beiden Rückenflossen ermöglicht. Diese wurden erst kürzlich erstmals detailliert beschrieben und vergleichend zwischen mehreren Haiarten und -familien analysiert. Da *Hemiscyllium ocellatum* nicht zu den untersuchten Präparaten zählt, wurde im Rahmen dieser Studie die Struktur und potenzielle Funktion dieser Muskulatur untersucht, basierend auf der Hypothese, dass sie eine Schlüsselrolle, bei der in Videoaufnahmen beobachteten, kontralateralen Rückenflossenbewegung während der Fortbewegung spielt. Die videoanalytische Auswertung umfasst eine schrittweise Beschreibung des Fortbewegungszyklus sowie eines neu identifizierten Bewegungsmusters während des Saugschnappens. Die Ergebnisse die Grundlage für zukünftige Studien der vergleichenden Morphologie sowie für eine vertiefte funktionelle Analyse der Lokomotion über alle Haifamilien hinweg.

# 1 Introduction

This thesis is divided into two parts: a comparative morphological study and a morphofunctional analysis. Each part is designed to stand independently and may be published separately in the future. The following introduction applies to both parts equally.

The origin of the class Chondrichthyes, the cartilaginous fishes, dates back approximately 450 million years (Andreev et al. 2015; Burrow et al. 2019). At this point in the evolutionary timeline, the classes Chondrichthyes and Osteichthyes diverged from each other (Brazeau & Friedman 2015; Grogan & Lund 2004; Grogan et al. 2012; Maisey 1996). Despite their considerable evolutionary history, cartilaginous fishes comprise a mere 4% of all extant fish species, the rest belongs to the Osteichthyes (Goldschmid 2014; Jabado et al. 2024). However, the cartilaginous fishes often play key roles in marine ecosystems, from pelagic apex predators to benthic dwellers (Carrier et al. 2022; Compagno et al. 2005). Today cartilaginous fishes comprise the Elasmobranchii and the Holocephali (Ebert et al. 2021; Nelson et al. 2016). While the Holocephali just include the chimaeras, with 60 species spread across three families (Fricke et al. 2025), the Elasmobranchii, containing all sharks, rays, and skates, makes up the vast majority of extant chondrichthyan species (Whitenack et al. 2022). Along with rays and skates (batoids) (831 species in 26 families), sharks (selachians) (607 species in 37 families) have particularly captivated the interest of researchers (Ebert et al. 2021; Fricke et al. 2025).

Sharks are currently classified into nine orders, i.e., Lamniformes, Carcharhiniformes, Orectolobiformes, Heterodontiformes (superorder Galeomorphii), Hexanchiformes, Squaliformes, Squatiniformes, Echinorhiniformes, and Pristiophoriformes (superorder Squalomorphii) (White et al. 2022). They have a variety of special characteristics in common including autapomorphic features typical for Chondrichthyes, such as a cartilaginous endoskeleton with superficial prismatic calcification (Goldschmid 2014; Maisey et al. 2021), and the presence of claspers (mixopterygia), which are modified extensions of the pelvic girdle in males, enabling internal fertilization (Grogan et al. 2012; Musick & Ellis 2005). Additional morphological characteristics are a cylindrical body shape, the presence of one or two dorsal fins, five to seven gill slits, and frequently a heterocercal caudal fin (Ebert et al. 2021). All nine orders show a broad ecological diversity, with species occupying a variety of aquatic habitats across the globe (Jabado et al. 2024). Some species, like *Carcharhinus leucas*

(Valenciennes, 1839) (bull shark), are capable of advancing into freshwater systems (Feitosa & Nunes 2020). Others even spend their entire life there, like members of the genus *Glyphis* (Last & Stevens 1994). Functionally, sharks have a high impact on ecosystems as meso- and apex predators (Compagno et al. 2005; Hammerschlag et al. 2025; Jabado et al. 2024; White et al. 2022), often exerting strong top-down regulatory effects (Baum & Worm 2009). Reflecting their ecological variability, there are also variations in locomotion and feeding types. Sharks of primarily pelagic orders (e.g., Lamniformes) are efficient long-distance swimmers mainly preying on mid- to upper-trophic level organisms (Cortes 1999) that are caught by ram-feeding (Frazzetta 1994; Motta & Wilga 2001). Few species are filter-feeders, like *Cetorhinus maximus* (Gunnerus, 1765) (basking shark) (Ebert et al. 2021). Benthic sharks often show a highly adapted morphology for benthic habitats and use suction feeding to capture their prey, as can be seen in most orectolobiforms (Goto 2001; Motta & Wilga 2001).

Orectolobiforms, or carpet sharks, are a relatively small group consisting of 45 extant species arranged into seven families (White et al. 2022). They are characterized by having nostrils with barbels that are connected through nasal grooves, a short mouth, and two spineless dorsal fins. As mentioned before, orectolobiforms have a benthic lifestyle, meaning that they live close to the ground, although the largest representative, the whale shark (*Rhincodon typus* Smith, 1828) is pelagic (Ebert et al. 2021; Rowat & Brooks 2012). Usually, orectolobiforms are found in depths up to 200m, with again the whale shark as an exception, reaching occasionally depths of almost 2000m (Weigmann 2016). Carpet sharks have a circum-tropical distribution, throughout warm-temperate and tropical waters, but are especially abundant in the Central Indo-Pacific (Ebert et al. 2021). Most Orectolobiformes feed on benthic crustaceans, fishes, cephalopods and molluscs, aligning with their bottom-dwelling lifestyle (Cortes 1999). For food intake, they rely on suction feeding, where they use a series of cranial muscles together with the pharyngeal cavity to generate a flow of water towards their mouth opening (Motta et al. 2008; Wilga & Sanford 2008). Due to their benthic orientation, many orectolobiforms developed a unique crawling locomotion, like the herein studied epaulette shark (Pridmore 1994).

The epaulette shark *Hemiscyllium ocellatum* (Bonnaterre, 1788), also known colloquially as “walking shark”, is a relatively small, benthic shark that reaches lengths up to 107 cm (Allen et al. 2016; Ebert et al. 2021). Its body is slender, elongated, and flexible, with a cylindrical trunk that continues into a caudal fin with a very distinct dorsal but reduced

ventral lobe. The pectoral and pelvic fins are adapted for “walking” locomotion and thus are relatively large and muscular (Goto et al. 1999; Pridmore 1994). The head has a short snout and is quite wide, with subterminal nostrils and two barbels anterior of the mouth opening. The five gill slits are small and positioned laterally posterior to the head (Allen et al. 2016; Ebert et al. 2021). Epaulette sharks are native to the tropical Western Pacific, from northern Australia to southern New Guinea, inhabiting the shallow coastal reef flats, lagoons, and tidal pools (Allen et al. 2016; Ebert et al. 2021; Last & Stevens 1994). They prefer complex reef structures, where they can seek shelter and hunt. Epaulette sharks are carnivorous benthic feeders, preying on small invertebrates and fishes, which are captured with the typical orectolobiform suction feeding (Motta & Wilga 2001). *Hemiscyllium ocellatum* exhibits a unique “walking” behaviour using coordinated movement of pectoral and pelvic fins (Pridmore 1994). This species has been observed to display a distinctive behaviour in which it is frequently observed to be either barely or not at all submerged and to "walk" over exposed reef tops during low tides (Heupel et al. 1999; Nay et al. 2021; Renshaw et al. 2002).

*Hemiscyllium ocellatum* is of high scientific interest due to its unique physiological and locomotor adaptations, even linking these features to the evolution of early tetrapods (Pridmore 1994). Pridmore (1994) described the three distinct gaits used while walking and swimming, which are also seen in neonates and juveniles (Porter et al. 2022). It tolerates extreme hypoxia and high temperatures, a trait likely linked to its ability to walk over exposed reef flats during low tides and hunt in tidal pools (Gervais et al. 2018; Heinrich et al. 2014; Heinrich et al. 2016; Renshaw et al. 2002; Routley et al. 2002; Wise et al. 1998). The paired fins exhibit morphological characteristics not observed in other elasmobranchs (Goto et al. 1999). Recently Medeiros et al. (2024) compared the *musculi inclinatores dorsales* across Galeomorphii but did not include *H. ocellatum*.

While these studies have provided valuable insights into specific anatomical aspects, a comprehensive, integrative understanding of the locomotor system of *H. ocellatum* is still lacking. Many investigations focus on isolated traits, often without placing them in a functional context. To date, no study has linked the detailed musculoskeletal anatomy with in vivo locomotor behaviour, underlining the need for integrative approaches combining anatomical data with behavioural observations. For instance, empirical evidence suggests a hitherto unobserved utilisation of the dorsal fins during walking and suction feeding, where

they bend in opposite directions, potentially implicating a locomotor function. This has not been described yet.

# 2 Goals

The primary objective of this study is to investigate the relationship between the musculoskeletal system and the observed walking-like locomotion in *H. ocellatum*. The movement primarily relies on its paired fins and is well adapted to the habitat in which the epaulette shark dwells. Another goal is to examine the specific motion sequence of the body during suction feeding in more detail and to investigate the role of the dorsal fins in this process. To address these objectives, the study features the following specific aims:

The first aim is the anatomical examination of *H. ocellatum* with a focus on skeletal und muscular components involved in locomotion. Since the pectoral and pelvic girdles have already been examined by Goto et al. (1999), the main focus is on the anatomy of the dorsal fins. The study of Medeiros et al. (2024) serves as a basis for this, which is to be expanded by the investigation of *H. ocellatum*. However, the methods used in the mentioned study are to be extended by micro-CT scans.

Secondly it is aimed to analyse the fin movements during locomotion and suction feeding based on in vivo video recordings. These observations will be used to describe the movement patterns of the fins, including the previously undocumented contralateral folding of both dorsal fins during walking and suction feeding.

The third aim is the integration of morphological and behavioural data to functionally interpret the locomotor system of *H. ocellatum*. The study aims to determine to what extent the anatomical structures can be linked to specific movement patterns, and if they can not only be interpreted as habitat-specific adaptations, but also as analogies to terrestrial locomotion. In this context, two hypotheses are proposed:

1. The morphology of the pectoral and pelvic girdle with the involved musculature in *H. ocellatum* reflects functional specialisations that facilitate a terrestrial-like mode of walking.
2. The dorsal fins are actively involved during walking locomotion and suction feeding, contributing to body stabilization, precise manoeuvring, and effective prey capture through postural control.

# 3 Material and Methods

Two life and two deceased specimens of *Hemiscyllium ocellatum* (Bonnaterre, 1788) (epaulette shark) were used in this study. The two life specimens comprising a male and a female are kept in the aquarium facility of the Evolutionary Morphology Research Group (EvoMoRG), located at the Department of Palaeontology of the University of Vienna. Two deceased specimens were provided for the study by Frederik Mollen from Elasmobranch Research Belgium (ERB), 2820 Bonheiden, Belgium. Both life specimens (EMRG-Chond-A-5, male; EMRG-Chond-H-2, female), have been determined to be in the subadult stage of development, with a total length of 66.78 centimetres in the male and 57.55 centimetres in the female. Both deceased specimen, male (EMRG-Chond-A-5) and female (EMRG-Chond-H-2), were stored refrigerated likewise at the Institute of Palaeontology.

## 3.1 Sample preparation

The female individual was used for the morphological investigation via dissection. It was therefore defrosted prior to and frozen after each examination step. The male specimen was kept frozen and only defrosted once to extract two transverse sections of the body at the level of the dorsal fins.

In preparation for micro-CT scanning, the transverse sections were placed within an airtight plastic container and submerged in 0,33% Lugol`s solution, which served a staining agent (Metscher 2009). The container was placed on a laboratory shaker (40 rotations per minute) and protected from light using an aluminium-container. A test scan was performed after three weeks, but the results did not match our expectations. None of the muscular structures were visible on the micro-CT scans. Following the scan the samples were put in a solution containing 50g of iodine per 1000ml of Alcohol (70%) to ensure greater iodine accumulation in the tissue and thus better visibility in the -micro-CT scan (Staggl et al. 2022) The final total storage time in the contrast medium was 40 days.

## 3.2 Dissection

Dissection continues to be one of the most important tools for anatomical research, primarily due to its hands-on nature (Elizondo-Omaña et al. 2005). It allows direct examination of tissue

properties like texture, flexibility, and the progression of individual fibres. The ability to manipulate the specimen during the process aids in understanding the function of joint-articulation and muscle action. Its biggest advantage over more “modern” methods is its relatively low cost in combination with the low equipment requirements. However, due to its destructive nature, it is only suitable for single use, which can be problematic for rare or limited specimen (Denton et al. 2018).

Dissection was performed according to the instructions of the dissection guide by (De Iuliis 2011). Progress was systematically documented using an iPhone 12 Pro and an iPhone 16 Pro mounted to a tripod to allow the subsequent morphological visualisation. For photography, the specimen was placed on a cutting pad with an integrated scale (Figure 1). The work was done step by step starting with one side only and leaving the other one intact for it to be used as a comparison. Starting with two incisions, one posterior the first dorsal fin and one posterior the gill opening, the skin was removed stepwise. Most of the connective tissue was detached together with the skin thereby exposing the outermost muscles and the ampullae of Lorenzini. In the next step, each muscle was removed individually starting from the head, continuing with the fins and ending with the torso and tail. Subsequently, the organs were removed, and the cartilaginous skeleton was uncovered. In the interest of avoiding potential damage, only a small part of the vertebral column was exposed from the covering connective tissue to permit adequate photo documentation.

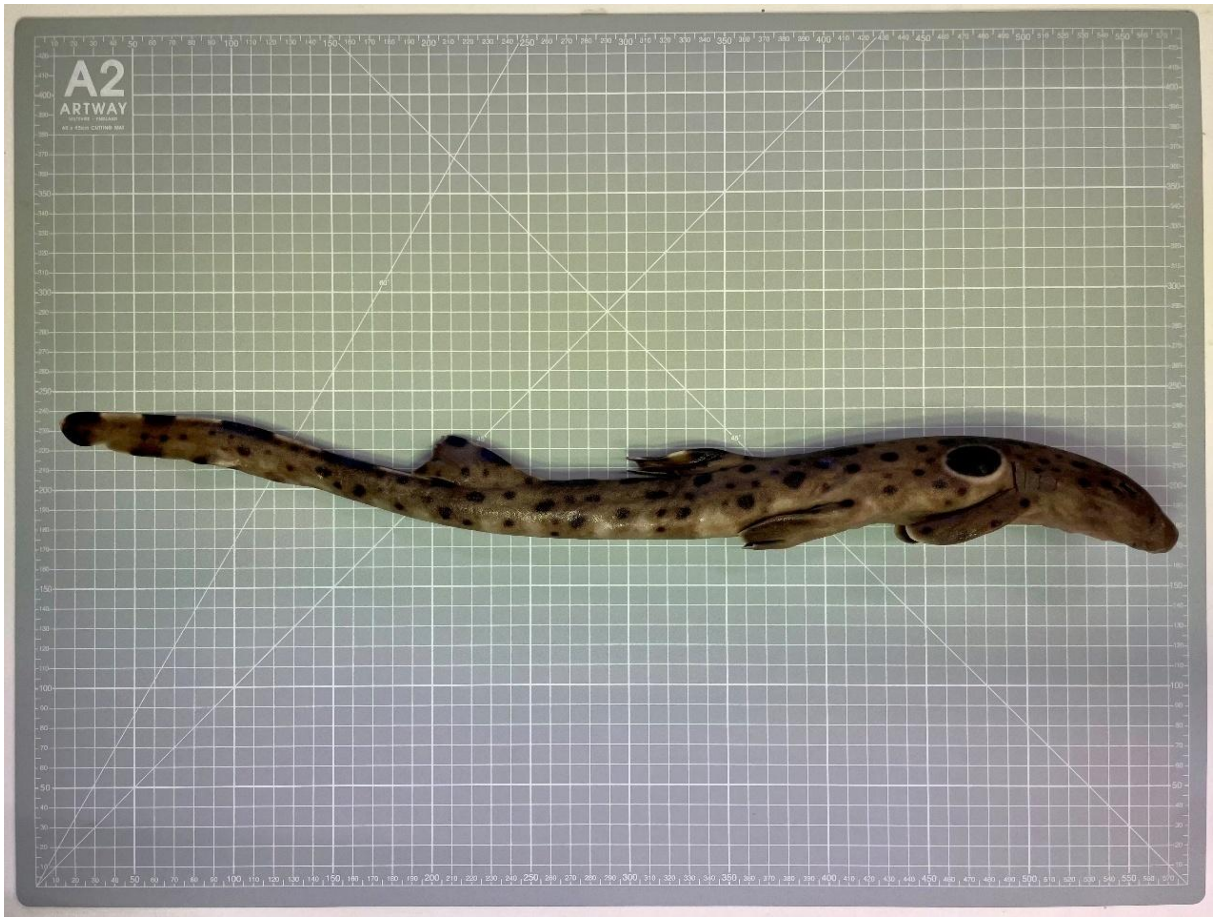


**Figure 1.** *Hemiscyllium ocellatum*, subadult female (EMRG-Chond-H-2): Lateral view on a cutting mat with scale (one square equals 1 cm edge length).

## 3.3 X-ray micro-computed tomography (micro-CT)

Micro-CT scanning is a non-destructive imaging technique that provides high-resolution, three-dimensional visualizations of both external and internal structures. It works similar to medical CT, but operating at a much finer scale, making it ideal for detailed anatomical studies (Keklikoglou et al. 2021). Both use an X-ray source that emits radiation, which subsequently passes through the object. During this process, the radiation gets absorbed or blocked by the tissue in a certain extent, depending on the density and composition of the material. The completed scan then depicts a picture in grey tones, in which lighter tones are to be interpreted as denser (e.g. bone, calcified cartilage) and darker tones as less dense (e.g. muscles, organs, uncalcified cartilage). Its main advantage, as opposed to dissection, is the preservation of specimens for future studies. However, it requires substantial technical resources and preparation time. A known limitation of micro-CT imaging is the poor contrast between different types of soft tissue (e.g. muscles, connective tissue) because of similar

radiodensity (Metscher 2009). This issue is addressed with DiceCT (diffusible iodine-based contrast-enhanced CT) (Gignac et al. 2016; Metscher 2009) Using iodine enriched samples (DiceCT), enables even more detailed scans. Due to the fact that iodine absorbs X-ray radiation, it allows to highlight tissues that enrich with iodine particularly easy.

The scans were conducted using a "SkyScan 1173 High Energy micro-CT" by Bruker using the parameters listed in Table 1. Its high spatial resolution makes it particularly suitable for morphological studies and comparative anatomical investigations (Gignac et al. 2016; Metscher 2009).

**Table 1.** Scanning parameters used for the micro-CT scans of the first and second dorsal fin of male specimen (EMRG-Chond-A-5)

| Sample | kV | mA | Exposure [ms] | Voxel size [µm] | Filter | Scanning time [min] | Number of images |
|---|---|---|---|---|---|---|---|
| First dorsal fin | 130 | 61 | 1180 | 35,763 | 0,25 mm brass | 1:59:32 | 1200 |
| Second dorsal fin | 130 | 61 | 1180 | 35,763 | 0,25 mm brass | 1:59:32 | 1200 |

The stained samples were wrapped in alcohol-soaked paper towels and packaged airtight using a layer of rubber to prevent drying out and shrinkage for micro-CT scanning. The results of the scan were then analysed qualitatively, and to allow a better understanding of the structures in focus, a few micro-CT images were selected for preparing figures.

**Figure 2.** *Hemiscyllium ocellatum*, subadult male (EMRG-Chond-A-5): Dorsal view with scale.

## 3.4 Image Processing

The acquired images from the dissection were edited and arranged as figures using Adobe Photoshop® CS6. Initially, a new project file (200 x 200 mm) with a black background layer was created. The individual photographs and micro-CT slices were pasted onto this background and arranged in logical context to each other, with changes in dimension and orientation made using the "*Transform tool"*. In a second step, the original picture scales were used to implement a standardised scale bar that could be placed next to the individual images for consistency. In a third step, the backgrounds of the individual images were removed using the "*Polygon Lasso"* tool. Selected sections and cropped segments of larger structures were outlined with a white frame. In a final step each photograph was labelled with a caption (e.g. a, b, c) to facilitate referencing within the text, and key anatomical features were indicated with arrows pointing from each structure to its corresponding abbreviation. This system allowed for clear cross-referencing between the text, the figures and the individual structures.

## 3.5 Video Recordings

While static anatomical methods provide detailed information about the structures involved in movement, they cannot capture the interaction and coordination of the individual structures during locomotion. Video analysis serves as a bridge between morphology and behaviour, allowing for the interpretation of movement patterns and linking them to the individual structures. To use them scientifically, video recordings must be conducted under laboratory conditions to allow easy replication. This includes the detailed documentation of all recording parameters (e.g. camera position, scale). The main advantage of this approach lies in its ability to document sequences of movement, providing the basis for kinematic analysis, like measuring the stride-length, step frequency, and the rotational parameters of limbs. In general, it allows the researcher to associate structures with actual motion patterns and to obtain a broad view of locomotion.

The two adult individuals were filmed in dorsal view using a GoPro Hero 12 Black, which was mounted above the tank using a clamp tripod (Figure 2). With the recordings their “walking”-locomotion and the movement patterns during suction feeding could be investigated as detailed as possible in a natural setting. Afterwards the video material was analysed qualitatively to be able to correlate the sequences of the paired and dorsal fins, and ultimately with the muscular and skeletal morphology.

**Figure 3.** Setup of video recording equipment using a clamp tripod mounted on the aquarium.

# 4 Comparative Morphology

## 4.1 Results

### 4.1.1 Methodology

Of the two specimens examined, dissection was performed only on the female, while the male was used for micro-CT examination. The initial treatment of the two body segments of the male specimen (EMRG-Chond-A-5) with contrast agent was 18 days in Lugol's solution. The first micro-CT scan after this time showed that only a small amount of iodine was able to accumulate in the inner tissues. Subsequently, an additional staining step was performed, during which the sample was immersed in a 50 g/L $H_2O$ iodine solution for 22 days. After storage in the higher concentrated solution, micro-CT scans showing several muscular and cartilaginous structures were successfully obtained. The different structures of the skin, musculature and cartilage skeleton could be clearly differentiated from each other by variation in different shades of grey. While more heavily calcified parts of the skeleton (e.g. neural process) and the musculature showed light grey tones due to higher density or iodine accumulation, connective tissue and less to barely calcified parts (e.g. dorsal fin radials) appeared in darker tones, since radiation just passes through them and iodine just accumulated on the edges. (Figure 4).

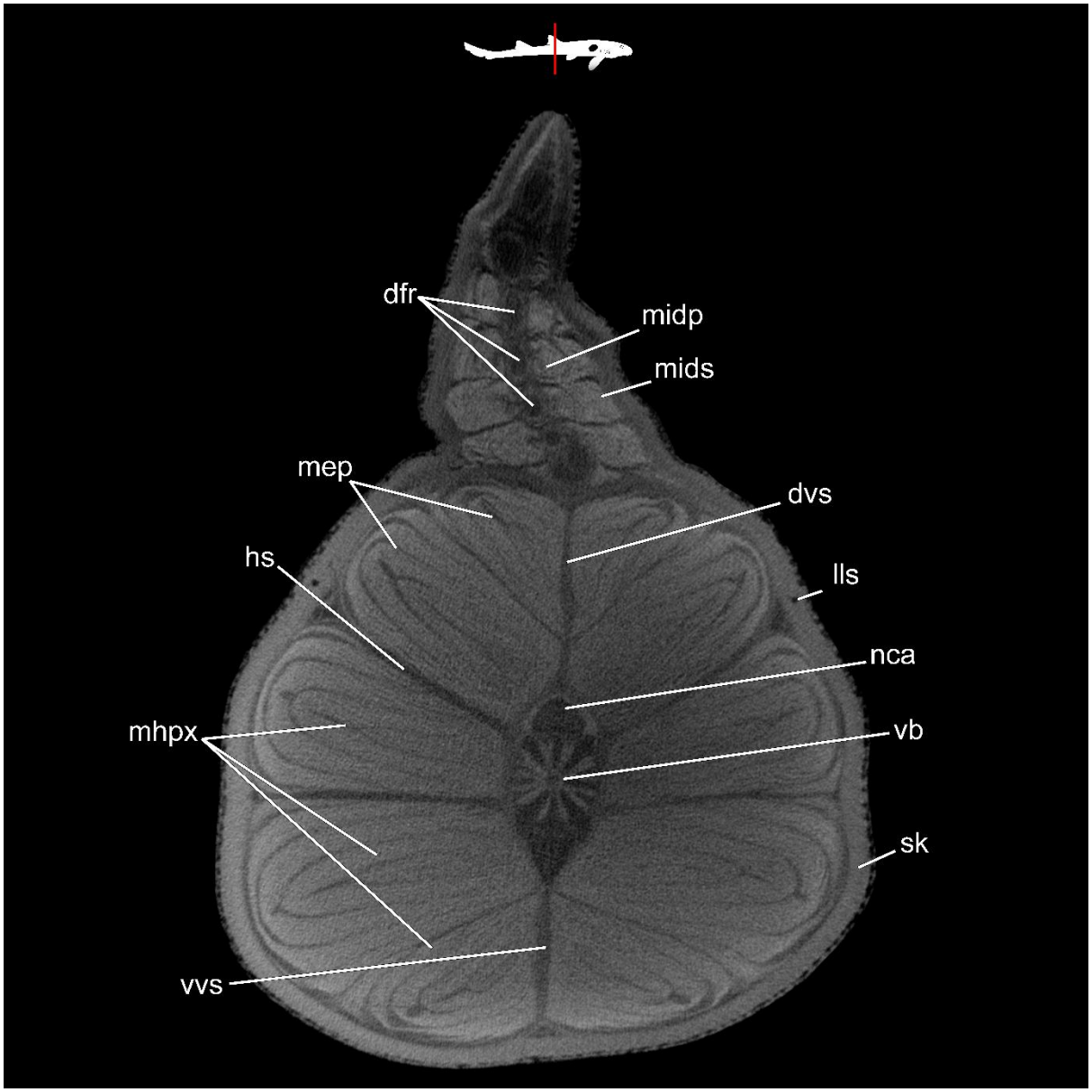


**Figure 4.** *Hemiscyllium ocellatum*, subadult male (EMRG-Chond-A-5): Micro-CT scan of precaudal tail including the first dorsal fin. Abbreviations: dfr, dorsal fin radials; dvs, dorsoventral septum; hs, horizontal septum; lls, lateral line system; mhpx, *musculus hypaxialis*; midp, *musculi inclinatores dorsales profundi*; mids, *musculi inclinatores dorsales superficiales*; nca, neural canal; sk, skin; vb, vertebral body; vvs, ventral vertical septum.

### 4.1.2 Morphology

The following pages present the results obtained through dissection, micro-CT imaging, and video analysis providing a detailed overview of the musculoskeletal system of *Hemiscyllium ocellatum* (Bonatterre, 1788). Subsequenly, these findings are compared with observations made on living specimens to relate specific anatomical structures to their functional roles.

When examining the two subadult individuals prior to dissection of the female (EMRG-Chond-H-2), the prominent large dark spots with white edges are most noticeable (Figures 2 and 5a,c). The coloration of the dorsal side of the body is of varying brown tones reaching from darker brown to a very light beige. The skin is characterised by a dark dotted pattern that extends from the head to the end of the caudal fin. The dots are less densely arranged on the rest of the body than on the head region anterior to the eyes and on the paired fins (Figures 2 and 5a,c). The ventral side is much brighter in colour showing a creamy white tone with no spots (Figure 4e). No sexual dimorphism is recognisable apart from the male claspers. Both the males and the females' body are elongated and cylindrical with a proportionally long, robust tail. In comparison to closely related species (e.g. *Chiloscyllium punctatum*) (Staggl et al. 2022) the heads appear narrower and rounder, but still being dorso-ventrally flattened with a ventrally pointing snout, which is clearly visible in lateral view. The mouth opening, labial folds, the paired barbels and the nostrils are visible in ventral view (Figures 5e and 7b). Also, some of the very small teeth from the upper and lower jaw are visible. Five gill openings are situated laterally at the height of the pectoral fin, with the gill apparatus drawing under the Chondrocranium. The fourth and fifth gill opening are situated very close together (Figures 5c and 7c). In dorsal and lateral views, the relatively large eyes and right behind them the spiracles can be seen. The eyes are positioned more dorsally compared to pelagic sharks (Figures 5c and 7a,c). In the ventral, dorsal and lateral regions, pores are arranged in rows, however, they are hardly visible. The pattern is best observed when the skin is removed. (Figure 7a,c). The caudal fin is strongly heterocercal with a distinct dorsal lobe. The lobe exhibits two notches: the more posterior subterminal notch and a notch separating the caudal from anal fin (Figures 5c,d,e,f and 6a,b). Both dorsal fins are positioned further back on the body, compared to pelagic species, with the first dorsal fin being located posterior to the height of the pelvic fins (Figure 5c,d). Both the pectoral and pelvic fins are relatively large and muscular in relation to the body size (Figure 5e,f).

The removal of the skin, which was largely detached along with the underlying connective tissue, reveals the musculature below. Due to strong adhesion, the removal of the skin from the fins was especially challenging. The ampullae of Lorenzini are visible on the head when the skin is removed. Especially on the dorsal and lateral side of the rostral region, a curved pattern of the ampullae is well discernible (Figure 7a,c) The ampullae of Lorenzini are connected through channels, which in turn are connected to the environment through the previously mentioned pores on the skin. According to papers by (Gauthier et al. 2019; Winther-Janson et al. 2012), these channels spread over the head and body in specific patterns. A posterior channel divides into the supratemporal, the infraorbital and the supraorbital channels. The infraorbital splits again into a mandibular and a hyomandibular channel. On the dorsal part, a median and a nasal channel is situated (Figures 7a,c and 8a,c).

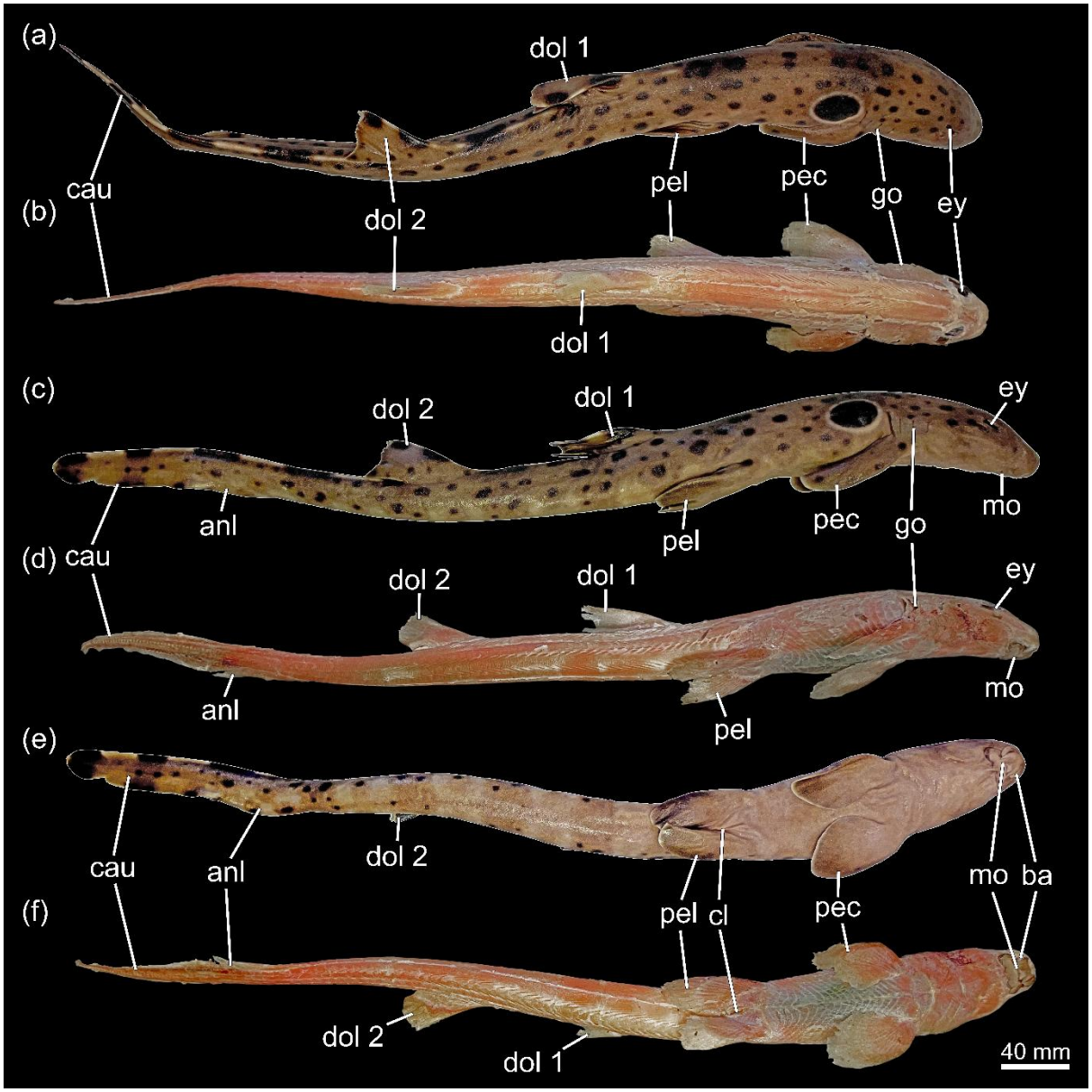


**Figure 5.** *Hemiscyllium ocellatum*, subadult female (EMRG-Chond-H-2): Different perspective of the whole body with and without skin. (a) dorsal view showing the epaulette spot, (b) dorsal view without skin, (c) lateral view, (d) ventral view without skin , (e) ventral view, and (f) ventral view without skin. Abbreviations: anl, anal fin; ba, barbell; cau, caudal fin; cl, cloaca; dol 1, first dorsal fin; dol 2, second dorsal fin; ey, eye; go, gill opening; mo, mouth opening; pec, pectoral fin; pel, pelvical fin.

#### *4.1.2.1 Locomotory muscles*

##### 4.1.2.1.1 Musculus epaxialis and musculus hypaxialis

The *musculus epaxialis* is one of the two most prominent muscles, that extend over most of the body. The two strands from the epaxial muscles originate at the chondrocranium just posterior to the eyes and run dorsal to the horizontal septum, that separates it from the *musculus hypaxialis* (Figure 13b,c), and dorsolateral to the vertebral column. It reaches into the caudal fin (Figures 5b,d and 7a). In general, the two strands appear as a single, massive bundle with the exception of the precaudal region (anterior to the caudal peduncle, where they are separated by the neural arches of the vertebral column (Goto 2001). Consequently, as one moves posteriorly, the muscle strands become progressively thinner (Figures 5b,d, 6b and 7b). The *musculus hypaxialis* runs below the above-mentioned horizontal septum forming a single strand. At the ventral side of the body, it forms a thin layer surrounding the abdominal cavity (Figures 5f and 7b,c). The posterior portion of *musculus hypaxialis* becomes a single longitudinal strand similar to the *musculus epaxialis* (Goto 2001).

##### 4.1.2.1.2 Musculus radialis

On the ventral side of the caudal fin, a small longitudinal muscle can be found. The *musculus radialis*, formerly referred to as *musculus flexor caudalis* (Goto 2001), originates at the end of the anal fin at the height of the notch separating it from the caudal fin. It extends to the end of the vertebral column (Figure 6b) (Flammang 2010; Goto 2001).

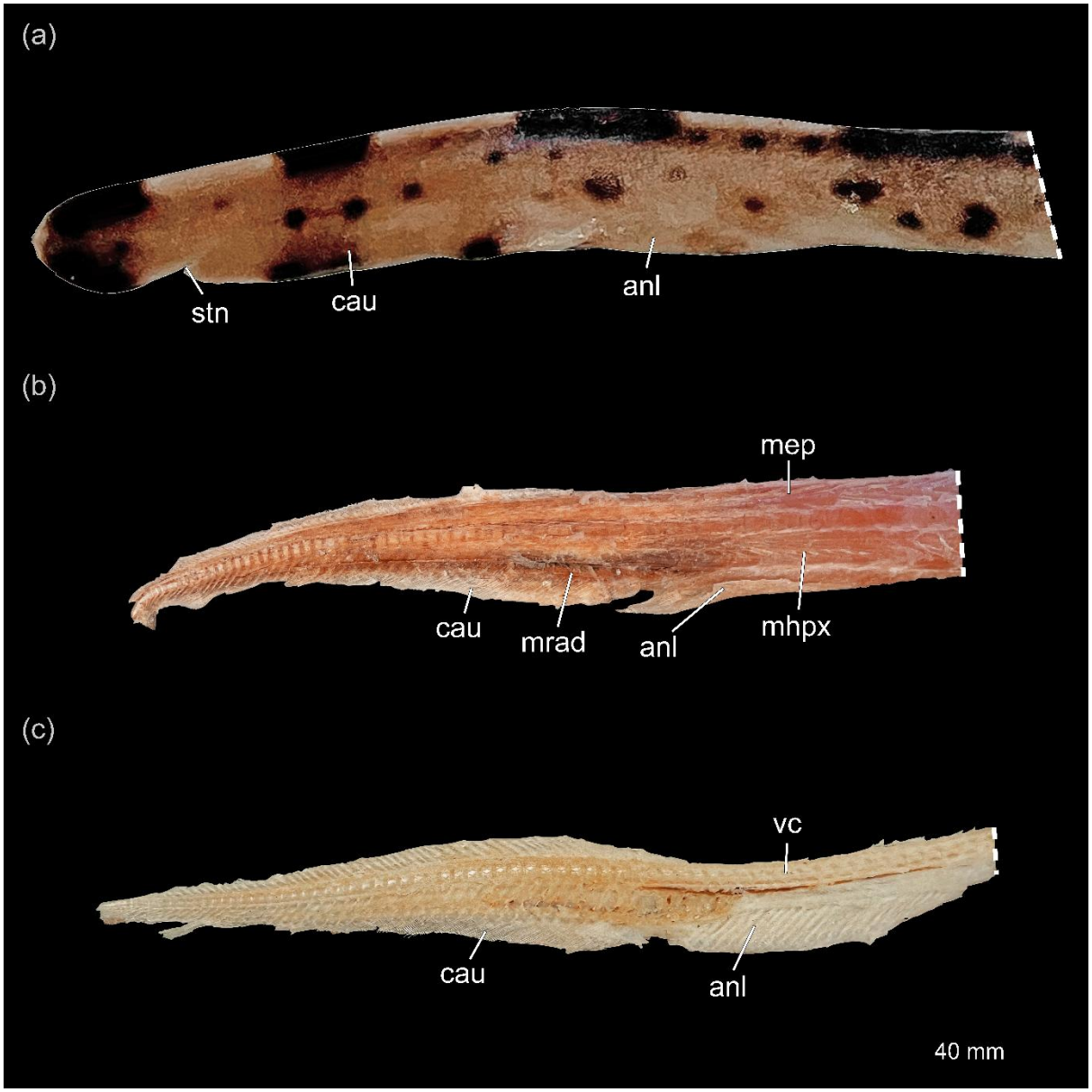


**Figure 6.** *Hemiscyllium ocellatum*, subadult female (EMRG-Chond-H-2): Lateral views of caudal fin throughout the dissection process. (a) with skin, (b) muscluar system, and (c) cartilaginous skeleton. Abbreviations: anl, anal fin; cau, caudal fin; mep, *musculus epaxialis*; mhpx, *musculus hypaxialis*; stn, subterminal notch; vc, vertebral column.

#### *4.1.2.2 Cranial musculature*

The cranial muscles of *Hemiscyllium ocellatum* primarily serve the movement of jaws, eyes and gills. They are assigned to the seven visceral arches, i.e., mandibular, hyoid and five branchial arches (Goto 2001).

##### 4.1.2.2.1 Mandibular arch

The muscles involved in the orectolobiform mandibular arch are the *musculus adductor mandibulae*, the *musculus suborbitalis*, the *musculus constrictor dorsalis*, the *musculus spiracularis* and the *musculus intermandibularis* (Goto 2001).

###### *4.1.2.2.1.1 Musculus adductor mandibulae*

The *musculus adductor mandibulae* or jaw adductor is a massive muscle that connects parts of the Meckel's cartilage with the palatoquadrate. It orientates on the dorsoventral side of the shark's head (Figures 7b,c and 8a). According to Goto (2001)and Soares and Carvalho (2013), the muscle consists of four parts, i.e., *musculus adductor mandibulae I-IV*, from anterior to posterior, with different orientations of the individual muscle fibres in Orectolobiformes. The *musculus adductor mandibulae I* originates on the distal surface of the Meckel's cartilage and inserts on the *musculus suborbitalis* (Figure 8b,c) (Goto 2001). The *musculus adductor mandibulae II* and *III* are positioned anterior to the *musculus adductor mandibulae I*. The *musculus adductor mandibulae* II is situated in the posterodorsal region of the muscle complex and mainly attaches to the palatoquadratum. The *musculus adductor mandibulae III* is the largest portion and situated in the posteroventral region, where it connects to both, the palatoquadratum and the Meckel's cartilage. The *musculus adductor mandibulae IV* is separated from the *musculus adductor mandibulae III* and covers the quadratomandibular joint. It inserts at the connective tissue covering the muscle complex (Goto 2001).

###### *4.1.2.2.1.2 Musculus suborbitalis*

The *musculus suborbitalis*, which also is called *preorbitalis* or *musculus levator labii* (Mallatt 1996) is strongly attached to the dorsal side of the chondrocranium and is part of the adductor-mandibular-complex (Soares & Carvalho 2013). Dorsally it originates from the ethmoid region of the neurocranium and protrudes over the cranium, where it comes in

contact with the *musculus epaxialis*. They remain separated by connective tissue (Figure 7a). From a lateral view the *musculus suborbitalis* surrounds the anterior part of the orbita, overlaps the palatoquadratum, and inserts at the Meckel's cartilage (Figures 7c and 8a,b,c) (Goto 2001).

##### *4.1.2.2.1.3 Musculus constrictor dorsalis*

It was not possible to expose the *musculus constrictor dorsalis* without causing significant damage to the muscle, which would have rendered it impossible to recognise. In *Chiloscylium punctatum* and *Hemiscyllium ocellatum* the *musculus constrictor dorsalis* consists of up to two parts, i.e., the *musculus levator palatoquadrati* and the *musculus spiracularis* (Goto 2001); (Soares & Carvalho 2013). In *Chiloscyllium plagiosum*, the *musculus levator palatoquadrati* originates from the postorbital process and inserts on the lingual surface of the palatoquadratum (Goto 2001). The *musculus spiracularis* originates from the lateral wall of the otic capsule just posterior to the *musculus levator palatoquadrati* and also inserts on the lingual surface of the palatoquadratum above where the palatoquadratum articulates with the Meckel's cartilage and on the wall of the spiracular cleft (Goto 2001). In *Chiloscylium punctatum*, a close relative to *Hemsicyllium ocellatum*, the *musculus levator palatoquadrati* conversely runs on the inside and the *musculus spiracularis* on the outside (Staggl et al. 2022).

##### *4.1.2.2.1.4 Musculus intermandibularis*

The paired *musculus intermandibularis* originates at subcutaneous tissue of the *musculus genio-coracoideus*. The two muscle strands of the *musculus intermandibularis* fuse in the anterior region (Figure 7b). It inserts along the ventral surface of the Meckel's cartilage (Figure 7b). From the point of fusion it runs diagonal to the body axis and has a tight connection to the *musculus constrictor hyoideus* ventralis (Figure 7b) (Goto 2001; Soares & Carvalho 2013).

#### 4.1.2.2.2 Hyoid arch

The muscles of the hyoid arch consisting of basihyale, ceratohyale, and hyomandibula in Orectolobiformes include the *musculus constrictor hyoideus dorsalis* and *musculus constrictor hyoideus ventralis* (Goto 2001).

#### *4.1.2.2.2.1 Musculus constrictor hyoideus*

The *musculus constrictor hyoideus* is composed of two portions, the *musculus constrictor hyoideus dorsalis* and *ventralis* (Goto 2001). The dorsal part is subdivided into the *musculus constrictor hyoideus dorsalis* and the *musculus levator hyomandibulae*. The first one originates on the posterodorsal surface of the otic capsule and the lateral surface of the *musculus epaxialis*. It is inserting at the hyomandibula. The second one originates from the posterodrosal surface of the otic capsule and attaches to the lateroventral part of the hyomandibula (Figure 8a,b,c) (Goto 2001; Soares & Carvalho 2013). The *musculus constrictor hyoideus dorsalis* superficially covers parts from the first branchial arch (Figures 7c and 8a). In ventral view, the *musculus constrictor hyoideus ventralis* originates from the subcutaneous tissue at the lateral edge of the Meckel's cartilage (Soares & Carvalho 2013) and inserts on the ceratohyale (Figures 7b,c) (Goto 2001). In the branchial region, the *musculus constrictor hyoideus dorsalis* and *musculus constrictor hyoideus ventralis* are fused (Figure 7c).

### 4.1.2.2.3 Hypobranchial muscles

In orectolobiforms, the hypobranchial muscles consist of the *musculus genio-coracoideus*, *musculus rectus cervicis* and *musculus coraco-branchialis*. (Goto 2001).

#### *4.1.2.2.3.1 Musculus genio-coracoideus*

The *musculus genio-coracoideus* as a single bundle originates from the fascia of the *musculus coraco-hyoideus,* a part of the *musculus rectus cervicis*, and the aponeurotic septum and inserts on the ventral side of the Meckel's cartilage near the symphysis (Figures 7b,c,d and 8c) (Goto 2001).

#### *4.1.2.2.3.2 Musculus rectus cervicis*

The *musculus rectus cervicis* consists of two muscles, the *musculus coraco-arcualis* and the *musculus coraco-hyoideus*. The *musculus coraco-arcualis* is a paired muscle, with both strands originating from the anteroventral surface of the coracoid of the pectoral girdle (Figures 7b,d and 8c,). The *musculus coraco-hyoideus* originates from the anterior part of the *musculus coraco-arcualis* (separated by a septum) and the pericardial membrane (Figure 7d) and lies on the ventral side of the *musculus genio-coracoideus* (Figures 7d and 8c), fusing mesially (Goto 2001).

#### *4.1.2.2.3.3 Musculi coraco-branchiales*

The *musculi coraco-branchiales* generally are five pairs of muscles, corresponding to the five gill arches. They originate from the anterolateral surface of the coracoid and the pericardial membrane, and insert into the ventromedial side of the branchial arches (Goto 2001; Shirai 1992).

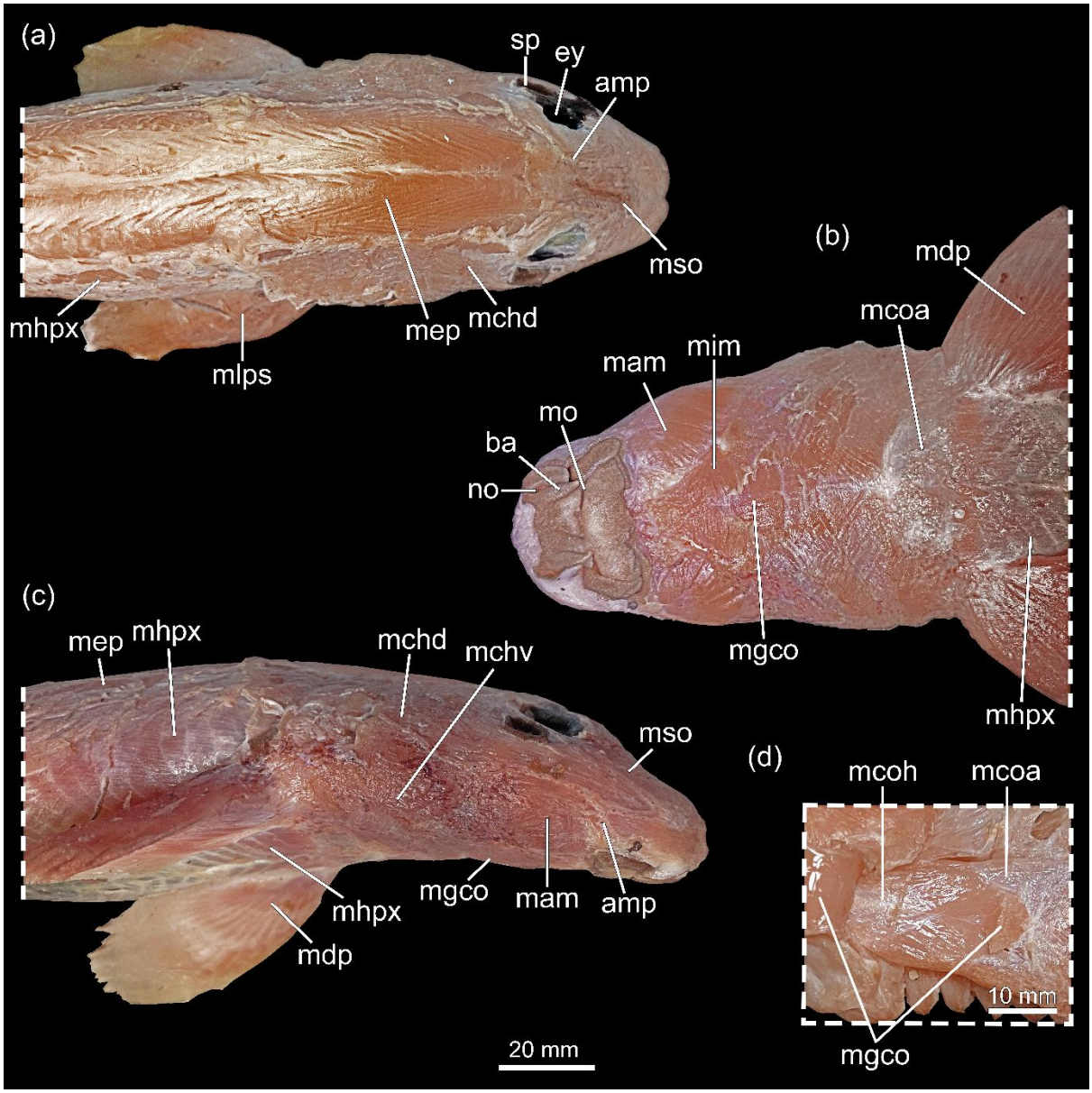


**Figure 7.** *Hemiscyllium ocellatum*, subadult female (EMRG-Chond-H-2): Different perspectives of the head region anterior to the pelvic girdle. (a) dorsal, (b) ventral, (c) dorsolateral, and (d) ventral detailed views. Abbreviations: amp, ampullae of Lorenzini; ba, barbell; ey, eye; mam, *musculus adductor mandibulae*; mchd, *musculus constrictor hyoideus dorsalis*; mchv, *musculus constrictor hyoideus ventralis*; mcoa, *musculus coraco arcualis*; mcoh, *musculus coraco-hyoideus*; mdp, *musculus depressor pectoralis*; mep, *musculus epaxialis*; mgco, *musculus genio coracoideus*; mhpx, *musculus hypaxialis*; mim, *musculus intermandibularis*; mlps, *musculus levator pectoralis superficialis*; mo mouth opening; mso, *musculus suborbitalis*; no, nostril; sp, spiracle.

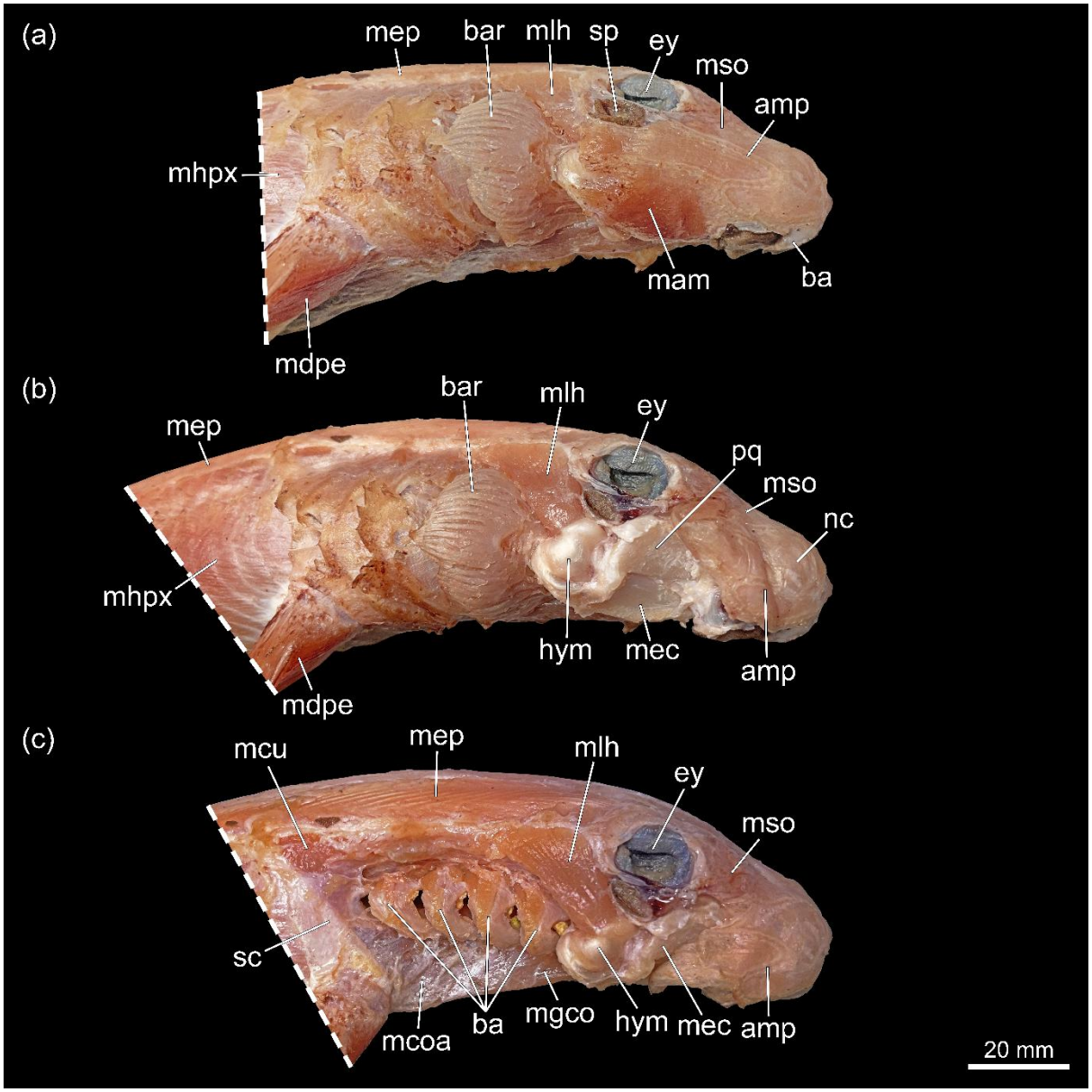


**Figure 8.** *Hemiscyllium ocellatum*, subadult female (EMRG-Chond-H-2): Different layers of the head region anterior of the pectoral girdle in lateral view. (a) removed *musculus constrictor hyoideus dorsalis*, (b) removed *musculus adductor mandibulae* and (c) exposed visceral arches. Abbreviations: amp, ampullae of Lorenzini; ba, barbell; ey, eye; hym, hyomandibula; mam, *musculus adductor mandibulae*; mchd, *musculus constrictor hyoideus dorsalis*; mcu, *musculus cucullaris*; mdpe, *musculus depressor pectoralis*; mec, Meckel's cartilage; mep, *musculus epaxialis*; mhpx, *musculus hypaxialis*, mlh, *musculus levator hyoideus*; mso, *musculus suborbitalis*; nc, nasal capsule, pq, palatoquadratum; sc, scapula; sp, spiracle.

#### *4.1.2.3 Pectoral muscles*

The pectoral muscles of *Hemiscyllium ocellatum* are supported by the pectoral girdle and the three basal cartilages of the pectoral fin, i.e., propterygium, metapterygium, and mesopterygium. As mentioned in the study by Pridmore (1994), the pectoral girdle in this species is capable of greater rotation than in other shark species. The muscles of the pectoral fins can be divided into the dorsal levator muscles and the ventral depressor muscles (Figure 9a,b,c,d) (Goto et al. 1999).

##### 4.1.2.3.1 Levator muscles

The levator muscle in *Hemiscyllium ocellatum* is divided into three layers, the *musculus levator pectoralis superficialis*, the *musculus levator pectoralis inferior* and the *musculus levator pectoralis distalis* (Figure 9b) (Goto et al. 1999).

###### *4.1.2.3.1.1 Musculus levator pectoralis superficialis*

The *musculus levator pectoralis superficialis* is the main dorsal elevator. It is the outermost, fan-shaped layer originating from the scapula. It covers the dorsal side of the mesopterygium, metapterygium and propterygium, the radials, as well as the two underlying muscle layers. It inserts on the radial cartilages (Figure 9a,b,d) (Goto et al. 1999).

###### *4.1.2.3.1.2 Musculus levator pectoralis inferior*

The *musculus levator pectoralis inferior* lies directly underneath the *musculus levator pectoralis superficialis* and in between the metapterygium and mesopterygium (Figure 9b). It is fan shaped too but due to its position not as wide as the layer above. It originates from the coracoid and inserts onto the posterior part of the mesopterygium (Goto et al. 1999).

###### *4.1.2.3.1.3 Musculus levator pectoralis distalis*

The *musculus levator pectoralis distalis* is a very thin muscle layer laying distal to the *musculus levator pectoralis inferior* (Figure 9b). It originates from the distal parts of the basal cartilages and inserts on the radial cartilages. Its dorsal part merges with the ventral part of the *musculus levator pectoralis superficialis* (Goto et al. 1999).

#### 4.1.2.3.2 Depressor muscle

The ventral side of the pectoral fins is made up by a single muscle, the *musculus depressor pectoralis*. It covers the ventral side of the mesopterygium, metapterygium and propterygium.

##### *4.1.2.3.2.1 Musculus depressor pectoralis*

The *musculus depressor pectoralis* is a fan-shaped muscle and thicker than its dorsal counterpart (Figure 9c,d). Furthermore, as one moves posteriorly, the muscle becomes increasingly massive. It extends over the dorsal part and in the anterior region to some extent over the lateral part of the pectoral fin (Figure 9d). The *musculus depressor pectoralis* originates from the coracoid and inserts onto the anterolateral parts of the mesopterygium and onto the radial cartilages (Goto et al. 1999).

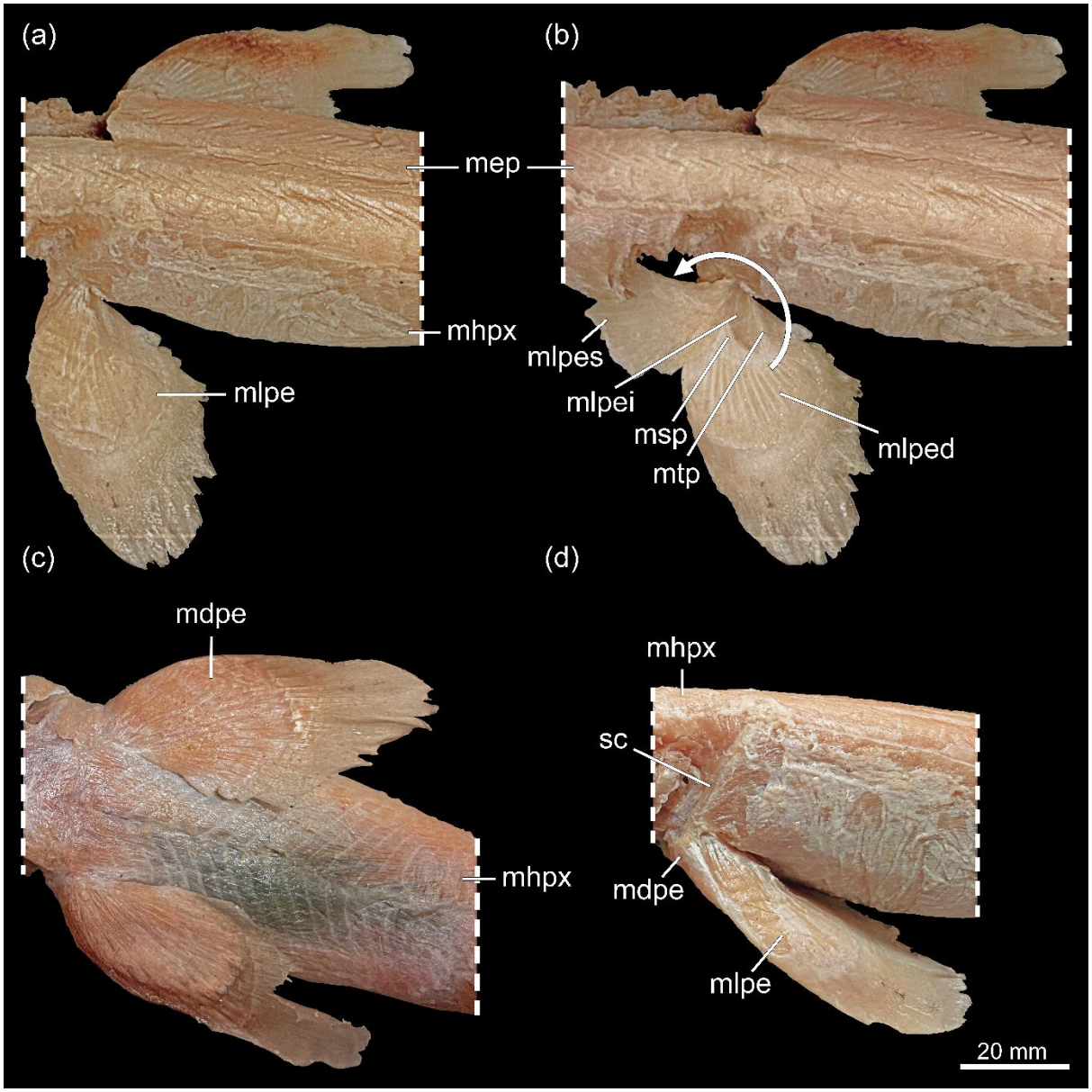


**Figure 9.** *Hemiscyllium ocellatum*, subadult female (EMRG-Chond-H-2): Different views on the pectoral girdle region. (a) dorsolateral, (b) dorsolateral with folded out *musculus levator pectoralis*, (c) ventral and (c) lateral view. Abbreviations: mdpe, *musculus depressor pectoralis*; mep, *musculus epaxialis*; mhpx, *musculus hypaxialis*; mlpe, *musculus levator pectoralis*; mlped, *musculus levator pectoralis distalis*; mlpei, *musculus depressor pectoralis inferior*; mlpes, *musculus levator pectoralis superficialis*; msp, mesopterygium; mtp, metapterygium; sc, scapula.

#### *4.1.2.4 Pelvic muscles*

The pelvic region of *Hemiscyllium ocellatum* consists of the pelvic girdle, the paired pelvic fins and, in males, the claspers (Goto et al. 1999). Similar as in the pectoral fins. the muscles of the pelvic fins include dorsal levator muscles and the lateral depressor muscles. Unlike the pectoral fins, a ventral adductor muscle is present (Figure 10 a,b,c) (Goto et al. 1999).

##### 4.1.2.4.1 Musculus levator pelvicus

The *musculus levator pelvicus* lies on the dorsal side of the pelvic fin and represents the most superficial layer (Figure 10a). It is a sheet-like muscle originating from the fascia of the hypaxial body muscle but remains distinct from the *musculus hypaxialis*. The muscle inserts on the dorsal side of the radial cartilages and the pelvic basipterygium (Goto et al. 1999). The muscle fibres span from the hypaxial body musculature to the fin and cover the underlying dorsal base of the pelvic fin (Figure 10a,b).

##### 4.1.2.4.2 Musculus depressor pelvicus

The *musculus depressor pelvicus* lies on the ventral side of the pelvic fin and is made up by two portions, an anterolateral and a posterolateral portion. The anterolateral part originates from the ventral surface of the prepelvic process and stretches over the anterior edge of the fin, where it appears as a robust bundle. Looking at the distal part of the fin, the second portion originates from the pelvic basipterygium and is thinner in structure. The *musculus depressor pelvicus* inserts on the anterior basal cartilages and the ventral side of the radials (Figure 10b,c) (Goto et al. 1999).

##### 4.1.2.4.3 Musculus adductor pelvicus

The *musculus adductor pelvicus* lies on the ventral, medial side of the pelvic fin. Anteriorly and distally, it is bordered by the *musculus depressor pelvicus* (Figure 10c). It originates from the ventral side of the puboischiadic bar and connective tissue of the ventral midline (Goto et al. 1999). It covers the pelvic fin radials and inserts onto the ventral side of the pelvic basipterygium (Goto et al. 1999).

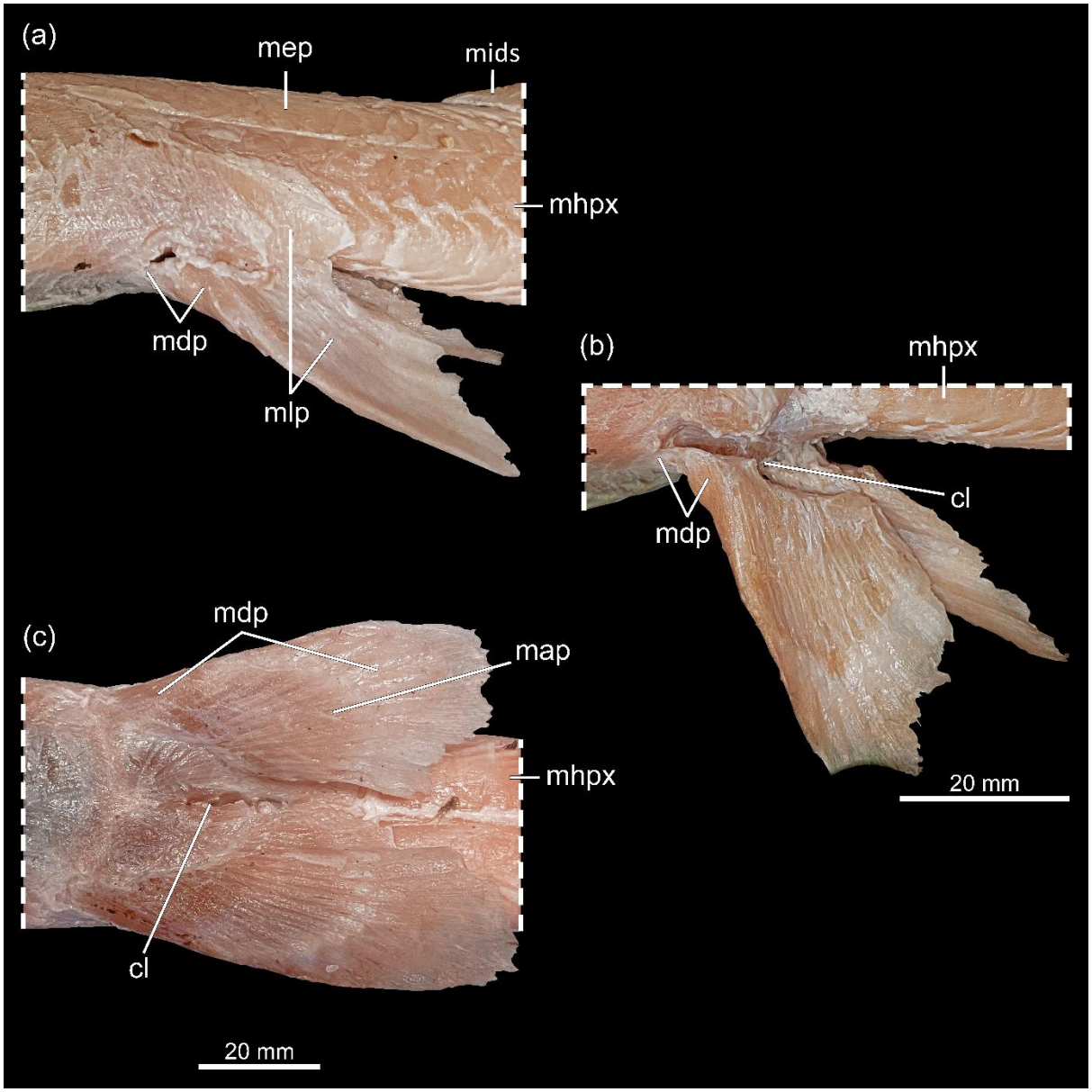


**Figure 10.** *Hemiscyllium ocellatum*, subadult female (EMRG-Chond-H-2): Different views on the pelvic region. (a) lateral, (b) lateral with removed *musculus levator pelvicus superficialis*, and (c) ventral. Abbreviations: cl, cloaca; map, *musculus adductor pelvicus*; mdp, *musculus depressor pelvicus*; mep, *musculus epaxialis*; mhpx, *musculus hypaxialis*; mids, *musculus inclinatores dorsales superficiales*; mlp, *musculus levator pelvicus*.

#### *4.1.2.5 Dorsal fin region*

##### 4.1.2.5.1 Muscles of the dorsal fins

The only muscles in the two dorsal fins of *Hemiscyllium ocellatum* are *the musculi inclinatores dorsales* (previously described as only a single muscle by (Goto 2001). They are divided into an outer layer, the *musculi inclinatores dorsales superficiales*, and an inner layer, the *musculi inclinatores dorsales profundi* (Figures 11 a,b,c and 12b,c) (Medeiros et al. 2024). While in some species the *musculi inclinatores dorsales profundi* reach in between the epaxial muscles and cover the dorsal fin basals in *Hemiscyllium ocellatum*, both of them have the same length and overlap completely (Figure 13b,c) (Medeiros et al. 2024). After the removal of the *musculus epaxialis*, it was possible to remove the dorsal fins, which was otherwise difficult, since the connective tissue surrounding the dorsal fin basals was attached to the *musculus epaxialis* (Figures 11a and 12a).

###### *4.1.2.5.1.1 Musculi inclinatores dorsales superficiales*

The *musculi inclinatores dorsales superficiales* cover the *musculi inclinatores dorsales profundi*, so that they were only visible by cutting into them and with the help of the micro-CT scan (Figures 11b,c, 12c and 13b,c). The adhesion between the two muscles is very strong, which made it difficult not separate them. Just a fine layer of connective tissue separates them. The border between the muscles is indicated with a red line in Figure 11c. In galeomorph sharks, the *musculi inclinatores dorsales superficiales* in general originate from an aponeurosis resting on the dorsal side of the musculus epaxialis and insert onto the fascia of the distal region of the *musculi inclinatores dorsales profundi* (Medeiros et al. 2024). Again, in all galeomorph sharks, the *musculi inclinatores dorsales* appear segmental, meaning that they are separated by the epimysium surrounding each muscle and to some extent and are also present in the free rear tip of the dorsal fins (Medeiros et al. 2024).

###### *4.1.2.5.1.2 Musculi inclinatores dorsales profundi*

The *musculi inclinatores dorsales profundi* lay directly beneath the *musculi inclinatores dorsales superficiales* and extend in between the radials (Figures 11b,c and 12c). They originate from the distal region of the fin basals and insert on the base of the distal radials (Medeiros et al. 2024).

#### 4.1.2.5.2 Cartilaginous skeleton of the dorsal fins

The skeleton of the dorsal fins is formed by two types, the dorsal fin basals positioned on the base of the fins and the dorsal fin radials located more distally. In *Hemiscyllium ocellatum*, the posterior basals and radials are fused, which is characterised by an apparent shortening of the basals (Figure 12d) (Goto 2001).

##### *4.1.2.5.2.1 Dorsal fin basals*

The dorsal fin basals penetrate the *musculus epaxialis* and are additionally enveloped by perichondrium, a sheath of connective tissue (Figures 11a,c and 12b,c). They are shorter than the radials (Figure 12d).

##### *4.1.2.5.2.2 Dorsal fin radials*

The dorsal fin radials consist of two cartilages, the proximal one being long and slender and the distal one being distinctly shorter, thicker, and in some cases, appear to be pointed (Figure 12d). They are embedded in the *musculi inclinatores dorsales profundi* (Medeiros et al. 2024).

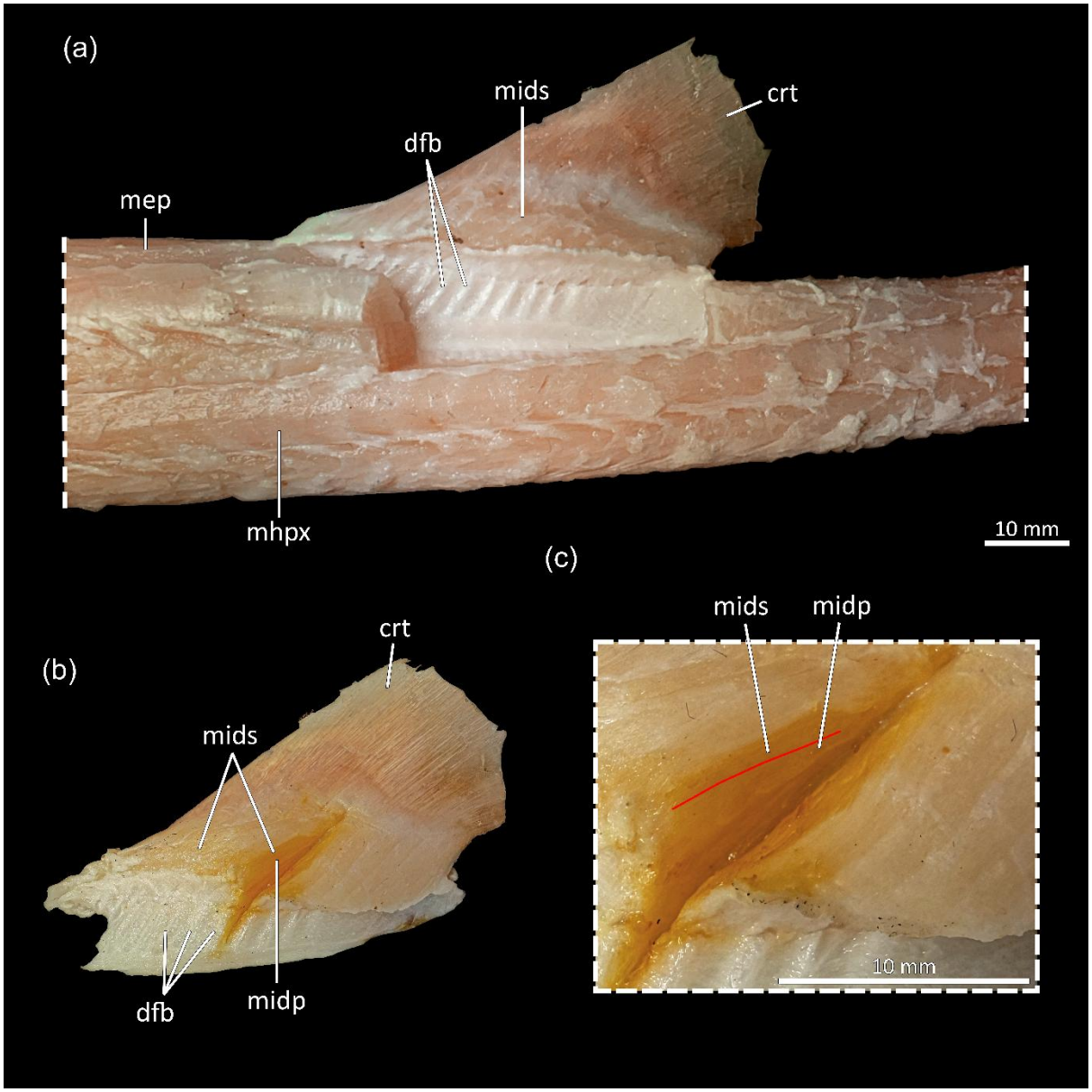


**Figure 11.** *Hemiscyllium ocellatum*, subadult female (EMRG-Chond-H-2): In situ, ex situ and detailed views of the second dorsal fin. (a) lateral in situ, (b) lateral ex situ and (c) detailed view. Abbreviations: crt, ceratotrichia; dfb, dorsal fin basals; mep, *musculus epaxialis*; mhpx, *musculus hypaxialis*; midp, *musculus inclinatores dorsales profundi*; mids, *musculus inclinatores dorsales superficiales*.

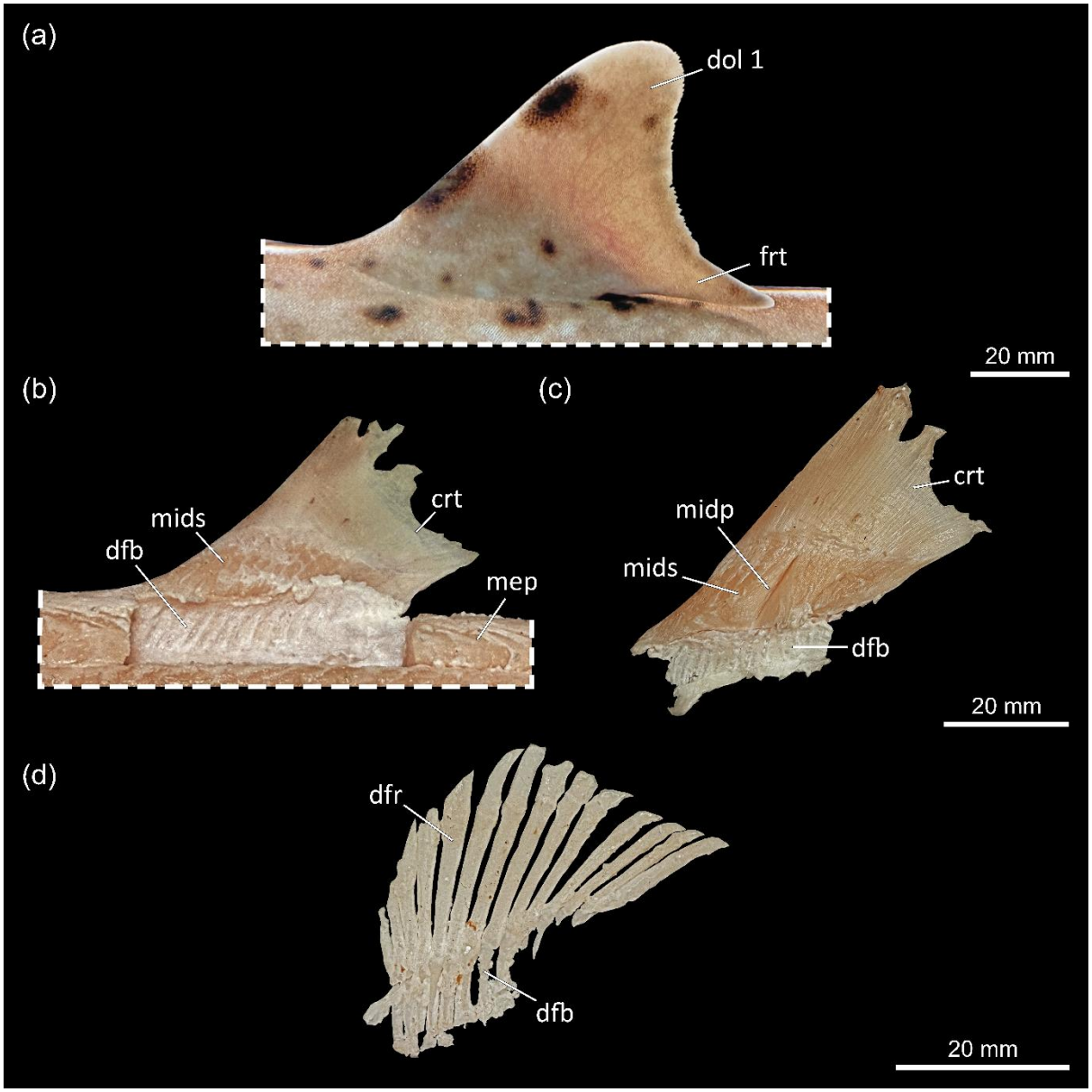


**Figure 12.** *Hemiscyllium ocellatum*, subadult female (EMRG-Chond-H-2): Different stages of the dissection of the first dorsal fin. (a) lateral in situ, (b) lateral in situ, (c) lateral ex situ and (d) lateral cartilaginous skeleton. Abbreviations: crt, ceratotrichia; dfb, dorsal fin basals; dfr, dorsal fin radials; dol 1, first dorsal fin; frt, free rear tip; mep, *musculus epaxialis*; midp, *musculi inclinatores dorsales profundi*; mids, *musculi inclinatores dorsales superficiales*.

#### *4.1.2.6 Dorsal fin cross section*

The micro-CT scan shows the details of the muscular and skeletal system of the male specimen (EMRG-Chond-A-5) of *Hemiscyllium ocellatum*. In the radio image showing the specimen in lateral view, the dorsal fin radials become visible (Figure 13a). The vertebral column, flanked dorsally by the *musculus epaxialis* and ventrally by the *musculus hypaxialis*, is visible with the neural arch positioned dorsally atop each vertebra and the haemal arch ventrally below. The cross sections of the micro-CT scan, one can see a transversal cut through the muscular and skeletal structures of the first and second dorsal fin region (Figure 13b,c). The most dorsal elements are the dorsal fins, with the dorsal fin rays (dark grey) being surrounded by the *musculi inclinatores dorsales*. When taking a closer look, the fine border between the *musculi inclinatores dorsales superficiales* and *musculi inclinatores dorsales profundi* becomes evident. Between the *musculi inclinatores dorsales* and the *musculus epaxialis*, a distinct aponeurosis is visible, serving as a tendinous boundary that separates these muscle groups The *musculus epaxialis* and *musculus hypaxialis* surround the vertebral column and the neural arch, being separated from another by the horizontal septum (Figure 13b,c). The two strands of the *musculus epaxialis* get separated by the dorsoventral septum and the *musculus hypaxialis* ventrally gets separated by the ventral vertical septum (Figure 13b,c). Embedded in the skin the ducts of the lateral line system can be seen (Figure 13b,c).

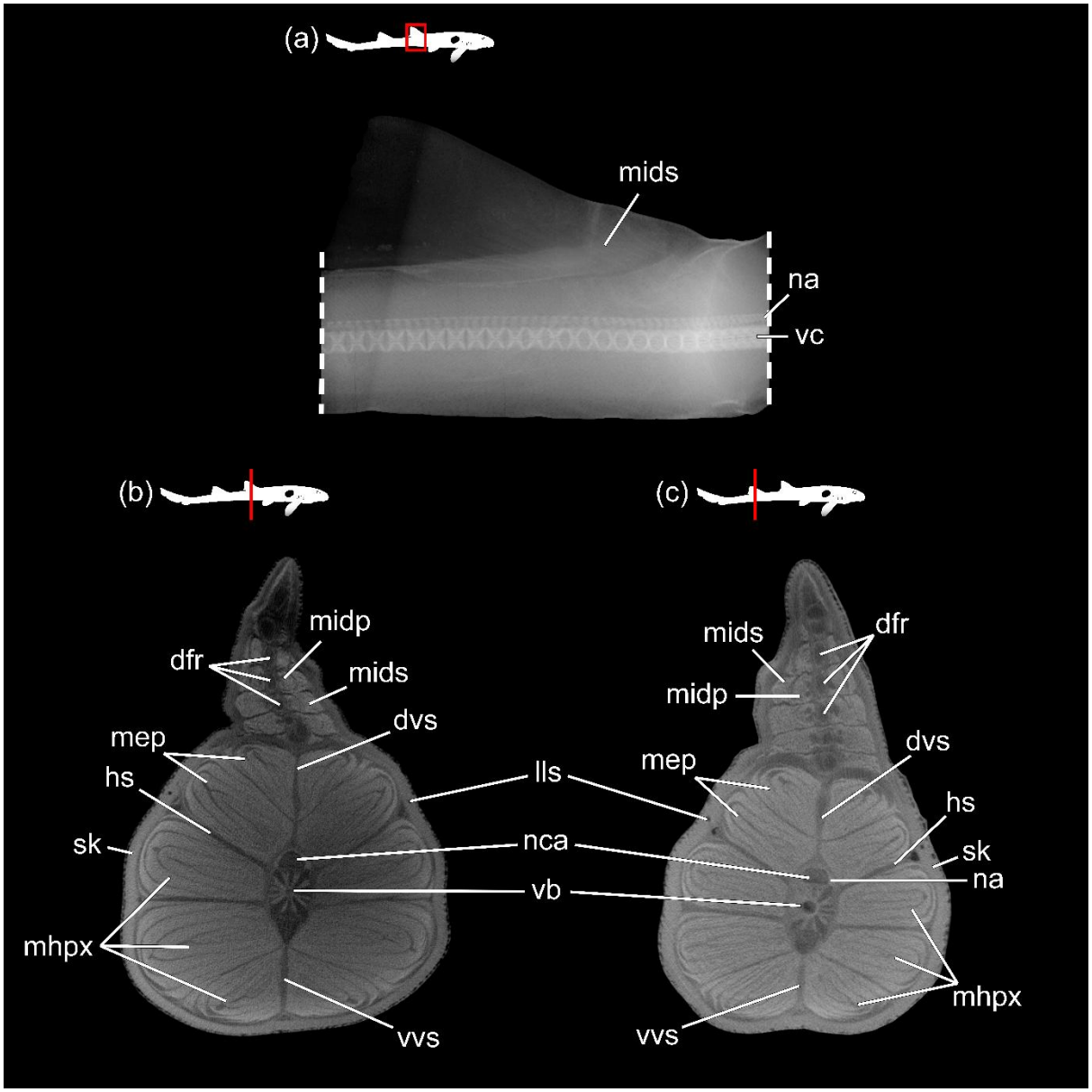


**Figure 13.** *Hemiscyllium ocellatum*, subadult male (EMRG-Chond-A-5): Micro-CT scans of the first and seconds dorsal fin regions. (a) radio image of first dorsal fin lateral, (b) first dorsal fin cross-section and (c) second dorsal fin cross-section. Abbreviations: dfr, dorsal fin radials; dvs, dorsoventral septum; hs, horizontal septum; lls, lateral line system; mhpx, *musculus hypaxialis*; midp, *musculi inclinatores dorsales profundi*; mids, *musculi inclinatores dorsales superficiales*; na, neural arch; sk, skin; vb, vertebral body; vc, vertebral column, vvs, ventral vertical septum.

#### *4.1.2.7 Cranial skeleton*

The skeletal parts of the head region of *Hemiscyllium ocellatum* consists of the chondrocranium, a seamless, moderately calcified capsule, that protects the brain and sensory organs, and the splanchnocranium, which is formed by seven visceral arches. The first arch, being the mandibular arch, the second one the hyoid arch and the third to seventh arch the branchial arches (Shirai 1992).

##### 4.1.2.7.1 Chondrocranium

The chondrocranium is a single large calcified cartilaginous capsule protecting the brain and sensory organs. It appears curved in lateral view, with an elongated anterior part (Figure 15e) that consists of a rostral process and paired nasal capsules containing the olfactory organ (Figure 15a,b,c). The most anterior tip of the chondrocranium is the rostral process that lies anterior to the internasal septum (Figure 15a,b,c,e). The nasal capsules themselves are somewhat globular, covered by connective tissue, and open anteriorly (Figure 14a,c). Internally, they are set apart by a thin internasal septum (Holmgren 1940). A large hole located medially on the dorsal side of the chondrocranium, the prefrontal fontanelle, is clearly visible (Figures 15a,c) (Goto 2001).

The orbital region contains two large eye sockets, the orbita, that form a large part of the skull of *Hemiscyllium ocellatum*. The orbita is positioned more dorsally in comparison to pelagic sharks, resulting in a more dorsolateral position of the eyes (Figure 15a,c,e) (Ebert et al. 2021). The dorsal margin of each orbita is the supraorbital crest, a reinforced ridge surrounding the dorsal and anterior part of the orbit (Figure 15a,e). The presence of multiple foramina in the orbital region enables the passage of nerves and blood vessels through the area. The most anterior positioned large foramen is for the cranial nerve II (nervus opticus) (Figure 15e; fII). Going further posterior, the foramen for the pituitary vein is positioned near the ventral edge of the chondrocranium (Figure 15e; fpit). Posterodorsal from it lies the big foramen for the cranial nerve V (nervus trigeminus) and VII (nervus facialis) almost at the posterior ridge of the orbita (Figure 15e; fV, fVII). The small foramen dorsal from it is for the superficial branch of the cranial nerve V (Figure 15c,e; $fV_{sup}$). The antorbital process is situated at the anterolateral end of the supraorbital crest and the postorbital crest extends on the posterior end of the orbita (Figure 15a,e). In dorsal view, the endolymphatic and

perilymphatic foramina are discernible on both sides of the chondrocranium near the lateral edges and at the height of the posterior ridge of the orbita (Figure 15a) (Goto 2001).

The otic and occipital region cover the posterior portion of the chondrocranium. The sphenopterotic ridge outlines the otic region dorsally and posteriorly (Figure 15d,e). The foramen for cranial nerve IX (nervus glossopharyngeus) is well visible on the posterior base of the sphenopterotic ridge (Figure 15e; fIX). In posterior view, the foramen magnum, which provides a passage for the spinal cord connecting the brain with the vertebral column and also provides a point of attachment for the vertebral column, is very prominent. The paired foramina for the cranial nerve X (nervus vagus) lie laterally of it on both sides (Figure 15d, fX) (Goto 2001).

Ventrally the chondrocranium is relatively flat with the antorbital ridge positioned at the height of the antorbital process. A paired foramina can be found below the orbital region (Figure 15b). As in most Orectolobiformes it fused from two separate foramina providing passage for the orbital and internal carotid artery (Goto 2001).

#### 4.1.2.7.2 Splanchnocranium

The splanchnocranium (or viscerocranium) is formed by a series of cartilaginous arches, the embryonic branchial arches, that later form the visceral arches (Miyake & McEachran 1991). In contrast to the unsegmented chondrocranium, the splanchnocranium is the only part of the skull that shows segmentation (Schilling & Thorogood 2000). As common in elasmobranchs, the splanchnocranium is superficially calcified (Ebert et al. 2021).

##### *4.1.2.7.2.1 Mandibular arch*

The mandibular arch robust, anteriorly extending and exhibits distinct adaptations for benthic feeding (Goto 2001). The two main parts of the mandibular arch are the paired palatoquadrate (upper jaw) and the paired Meckel's cartilage (lower jaw). In addition, three pairs of labial cartilages are present (Figure 14a,b,c). The upper jaw consists of two antimeres, the palatoquadrates, resting on the ventral side of the skull, meeting anteriorly along a vertical symphysis (Figure 14b,c). In lateral view, the palatoquadrate is slightly arched, appears massive on the posterior part, and tapering anteriorly. Centrally is a small elevation serving as an anchor point for the *musculus adductor mandibulae*, called the adductor

mandibular process. On the massive dorsal part of the palatoquadrate is another process pointing upward, the ascending process, which connects the palatoquadrate to the chondrocranium with a ligament, the ethmopalatine ligament (Figure 14c) (Goto 2001; Wilga 2005). On the anterior part of the jaw, facing ventral, a broad dental band can be located with the tiny teeth facing from labial to lingual (Goto 2001).

The lower jaw is a massive element again consisting of two paired elements, i.e., the Meckel's cartilages, which are connected along an oblique symphysis, which, unlike other genera of the Hemiscyllidae (e.g. *Parascyllium*, *Cirrhoscyllium*), composed only of connective tissue (Figure 14b,c). In lateral view, it is rather triangular shaped with a strong distal bend at the posterior end, the sustentaculum. On the dorsal end of the sustentaculum, it is connected to the palatoquadrate via the lateral part of the quadratomandibular joint (Figure (14c). The mandibular knob, a process serving as a connection to the hyomandibula, sits posterior to the quadratomandibular (Figure 24c) (Goto 2001). The dorsal side of the anterior part is bearing a dental band with teeth being arranged in labio-lingual aligned rows (Figure 14b) (Goto 2001).

Regarding the tooth morphology, Goto (2001) described them as being arranged in several rows, the labial rows containing the functional teeth, while the lingual rows represent the replacement teeth being still covered by tissue. The teeth themselves consist of a long medial cusp with a lateral cusp projecting on each side at the lower third of the tooth. The lateral cusps are reduced in size and oriented mesiodistally.

Two pairs of labial cartilages occur on the upper and one pair on the lower jaw (Figure 14b,c). The anterior upper labial cartilage attaches on the anterior part of the palatoquadrate and the posterior upper labial cartilage slightly posterior from it. The lower labial cartilage consists only of one element attaching to the Meckel's cartilage with a broadened end (Figure 14b) (Klimpfinger & Kriwet 2020).

#### *4.1.2.7.2.2 Hyoid arch*

The hyoid arch is positioned posterior to the mandibular arch and articulates at a number of points with it. It consists of five elements, i.e., an unpaired medial basihyale, paired ceratohyals, and paired hyomandibulas (Figure 14b,c).

The hyomandibula is a massive cartilage that connects the jaw to the chondrocranium, articulating with the anterior part of the ventral side of the mandibular knob, and to the side

of the cranium posterior to the otic capsule, in the hyomandibular fossa (Figure 14c) (Goto 2001).

The ceratohyale forms the elongated middle part of the hyoid arch, articulating posteriorly with the ventral part of the hyomandibula and anteriorly with the distal part of the basihyale (Figure 14c).

The unpaired basihyale forms a connection between the halves of the hyoid arch by articulating with both ceratohyales. It can be located at the base of the chondrocranium as an attachment point for the *musculus coraco-hyoideus* (Figure 14c).

#### *4.1.2.7.2.3 Branchial arches*

The five branchial arches are situated posteriorly to the hyoid arch. They are curved in a U-shape and form all together the branchial basket (Shirai 1992). Each branchial arche is composed of, from dorsal to ventral, paired pharyngobranchiales, paired epibranchiales, paired ceratobranchiales, paired hyporbranchiales and an unpaired basibranchiale (Figure 14a,b,c) (Goto 2001). The phayrongobranchiale is an elongated cartilage with a triangular pharyngobranchial blade (Goto 2001). It is dorsally connected to the vertebral column via connective tissue, forming the roof of the branchial basket. On its lateral facing tip, it connects to the shorter epibranchiale. The bifurcate gill pickaxe, or pharyngobranchial complex is formed by the fusion of the pharyngobranchiales of the last two gill arches with the epibranchiale of the last gill arch (Goto 2001) (Figure 14a). The distal end of the epibranchiale itself further articulates with the distal end of the ceratobranchiale, an elongated cartilage on the ventral side of the branchial basket representing the largest element of the gill arches (Figure 14b). The ceratobranchiales are connected medially to the corresponding hypobranchiale, from the third to fourth branchial arch. The two flattened basal cartilages to which all branchial arches are connected, are the single basihyale antero-ventrally and the single basibranchiale postero-ventrally. Anteriorly, the ceratobranchiale from the first gill arch articulates directly to the basihyale, the hypobranchiale is absent (Figure 14b). Further posteriorly, the hypobranchiale from gill arch two to four connect to the anterior margin of the basibranchiale (Figure 14b). The previously mentioned gill pickaxe from the fifth gill arch articulates with the lateral edge of the basibranchiale (Figure 14a,b,c). The branchial rays in *Hemiscyllium ocellatum* are, as in most orectolobiforms, slender and elongated (Goto 2001). They articulate with the epibranchiale and ceratobranchiale, with exception of the last gill

arch, where they only articulate with the ceratobranchiale, as the epibranchiale is part of the pharyngobranchial complex (Goto 2001). According to Goto (2001), orectolobiforms possess four or more branchial rays in the first four arches and less in the fifth gill arch (Figures 8a,b,c and 14a,b,c).

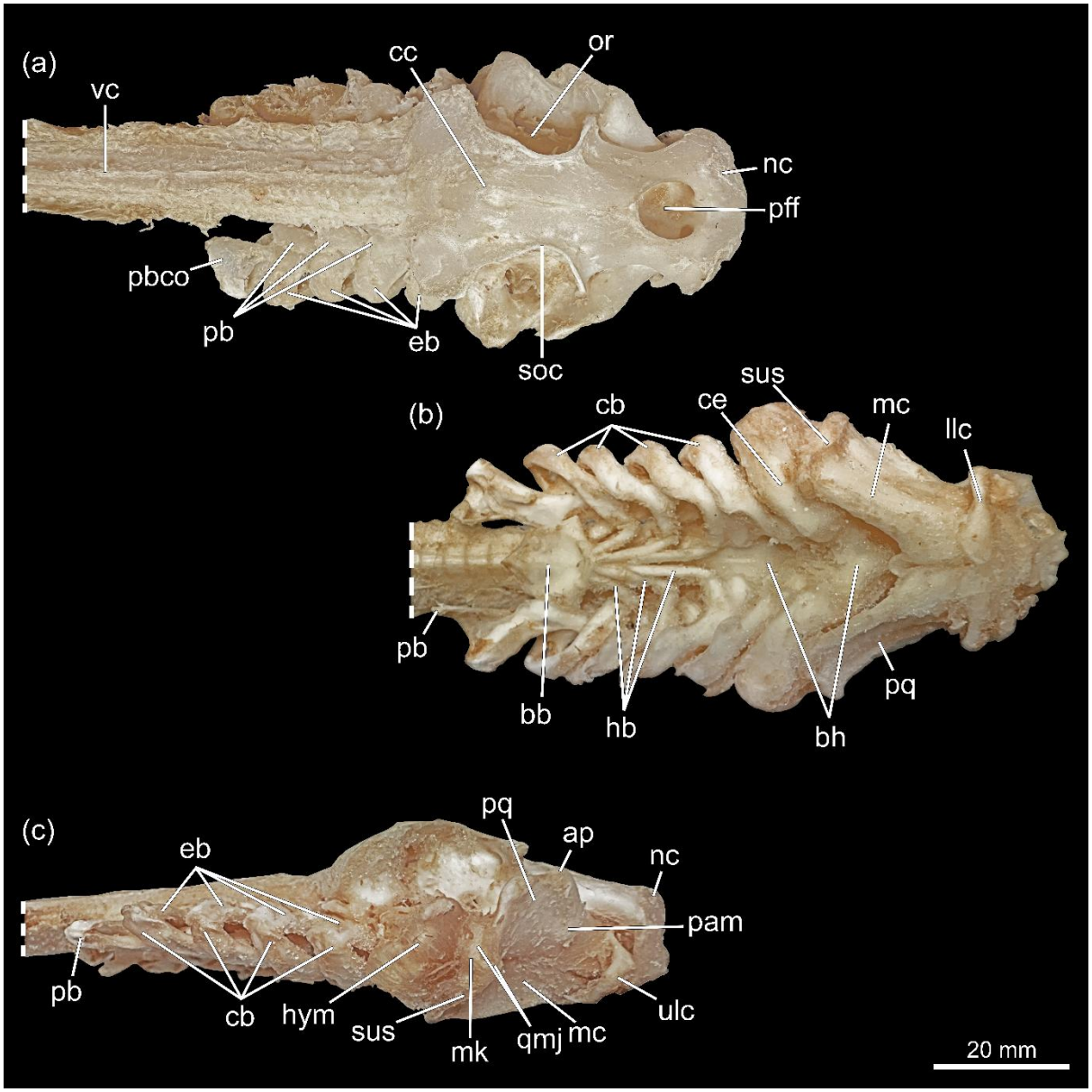


**Figure 14.** *Hemiscyllium ocellatum*, subadult female (EMRG-Chond-H-2): Different views of the Chondrocranium and the visceral arches. (a) dorsal, (b) ventral and (c) lateral view. Abbreviations: ap, ascending process; bb, basibranchiale; bh, basihyale; cb, ceratobranchiale; chondrocranium; ce, ceratohyale; be, epibranchiale; hb, hypobranchiale; hym, hyomandibula; llc, lower labial cartilage; mc, Meckel's cartilage; mk, mandibular knob; nc, nasal capsule; or, orbita; pam, processus for *musculus adductor mandibulae*; pb, pharyngobranchiale; pbco, pharyngobranchial complex; pff, praefrontal fontanelle; pq, palatoquadratum; qmj, quadratomandibular joint; soc, supraorbital crest; sus, sustentaculum; ulc, upper labial cartilage; vc, vertebral column.

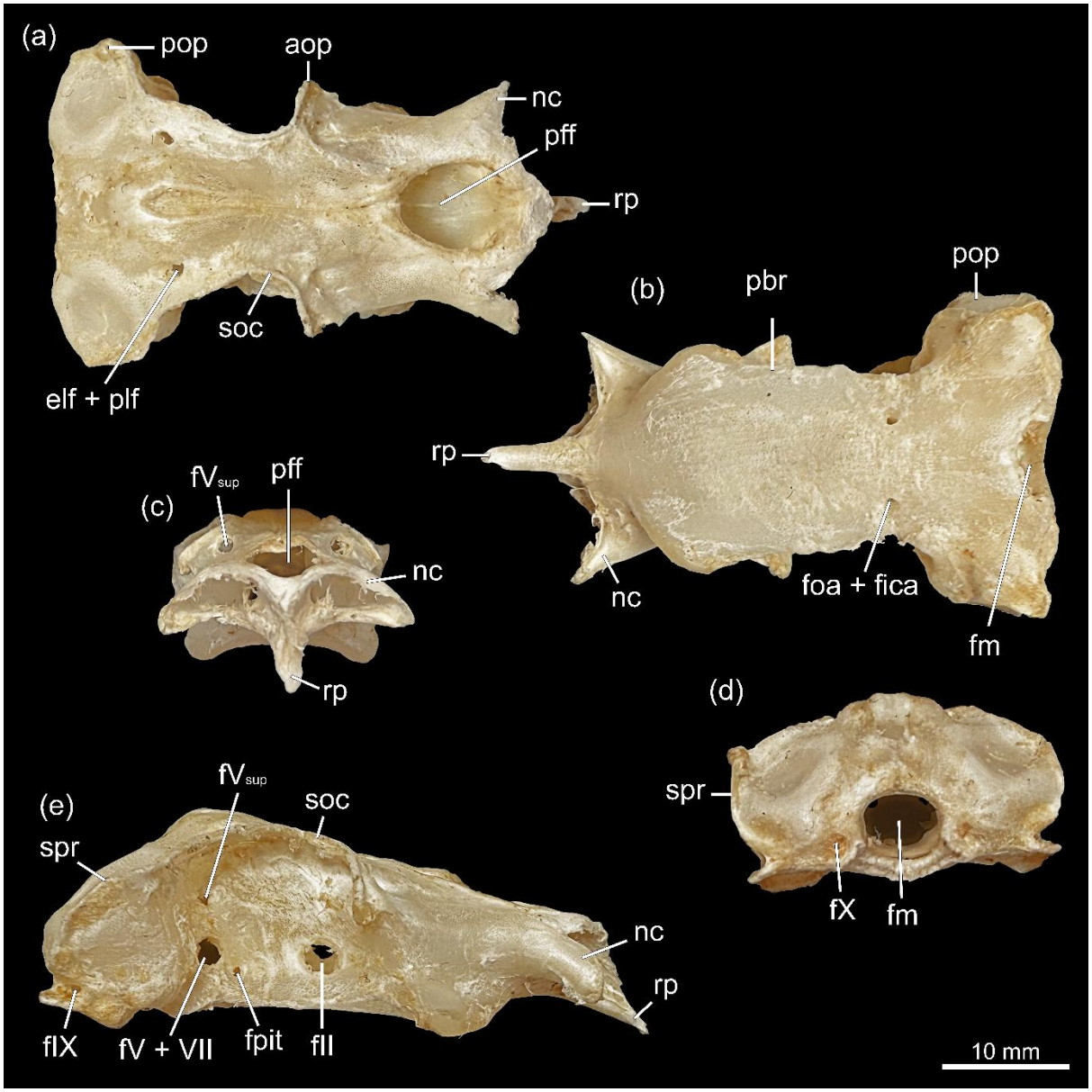


**Figure 15.** *Hemiscyllium ocellatum*, subadult female (EMRG-Chond-H-2): Different views of the Chondrocranium. (a) dorsal, (b) ventral, (c) frontal, (d) posterior and (e) lateral view. Abbreviations: aop, antorbital process; elf, endolymphatic foramen; fica, foramen of internal carotid artery; fII, foramen of cranial nerve II; fIX, foramen of cranial nerve IX; fm, foramen magnum, foa, foramen of orbital artery; fpit, foramen of pituitary vein; fVII, foramen of cranial nerve VII; $fV_{sup}$, foramen of superficial branch of cranial nerve V; fX, foramen of cranial nerve X; nca, neural canal; pbr, palatobasal ridge; pff, praefrontal fontanelle; plf, periymphatic foramen; pop, postorbital process; rp, rostral process; soc, supraorbital crest; spr, sphenopterotic ridge.

#### *4.1.2.8 Pectoral girdle*

The pectoral girdle of *Hemiscyllium ocellatum* consists of a fused scapulocoracoid, with a dorsal facing scapular process and the horizontal coracoid bar (Figure 16a,b). The whole structure is U-shaped with the apron sitting in the middle of the coracoid bar, supporting the pericardial cavity (Goto 2001). The pectoral girdle is tightly embedded into the body's musculature, with connective tissue providing a stable anchorage. Each side of the scapulocoracoid carries a pectoral fin that articulates laterally via an articular condyle that serves as a joint (Figure 16a,b) (Goto et al. 1999). In Orectolobiformes, like in most other shark orders, the pectoral fins usually consist of three basal cartilages, i.e., the propterygium, mesopterygium and metapterygium (Goto 2001). In *Hemiscyllium ocellatum*, the propterygium is fused with the mesopterygium, resulting in only two distinct basal cartilages, which are paddle-like shaped, elongated and broad (Figure 16a,b).

The pectoral fin radials that are articulating with the basals are positioned distally. The proximal radials connect directly to the basals, followed by the medial radials, that are in turn articulated with the distal radials (Figure 16a,b). But not all of them consist of three elements. According to Goto et al. (1999), the two anterior series are shorter and consist only of proximal and distal elements, while some of the posterior radial cartilages are missing the distal or medial elements (Figure 16a,b).

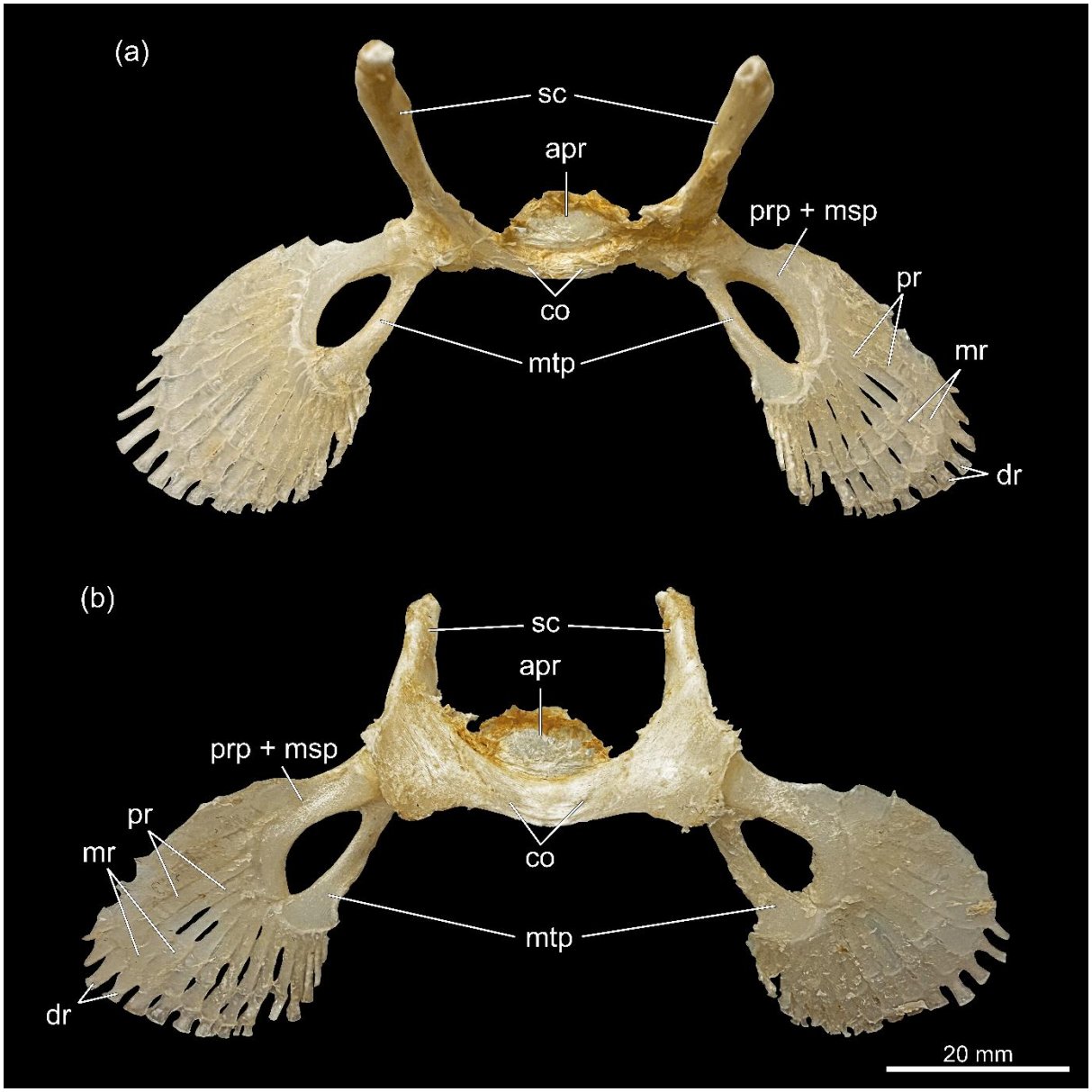


**Figure 16.** *Hemiscyllium ocellatum*, subadult female (EMRG-Chond-H-2): Different views of pectoral girdle. (a) dorsal and (b) ventral view. Abbreviations: apr, apron; co, coracoid; dr, distal radial; mr, medial radial; msp, mesopterygium; mtp, metapterygium; pr, proximal radial; prp, propterygium; sc, scapula.

#### *4.1.2.9 Pelvic girdle and fins*

The pelvic girdle of *Hemiscyllium ocellatum* consists of two parts, the puboischiadic bar, located ventrally in the body wall anterior to the cloaca, and the pelvic basipterygium (Figure 17a,b). The puboischiadic bar is slightly arched and fused into one continuous structure. Like the pectoral girdle, the pelvic girdle has no articulation to the vertebral column. A prepelvic process occurs at the anterolateral edges of the puboischiadic bar (Figure 17a,b). The basipterygium is a long, flattened and slightly bent cartilage positioned at the base of each pelvic fin (Figure 17a,b). All radials and the anterior pelvic basal cartilage are connected to it. In males, the basipteygium also supports the claspers (Goto et al. 1999). The anterior pelvic basal cartilage is the second one of the two basal cartilages (Figure 17a,b). Apart from the bifurcation mentioned by Goto et al. (1999) the anterior pelvic basal cartilage looks similar to the radials. The ridge implying the branching of the anterior pelvic basal cartilage is just slightly visible. During the dissection, one of them detached, which is why just one is present in Figure 17. The radials of the pelvic fins consist of two parts, i.e., the slender and very long proximal and the short, pointed distal radials (Figure 17a,b).

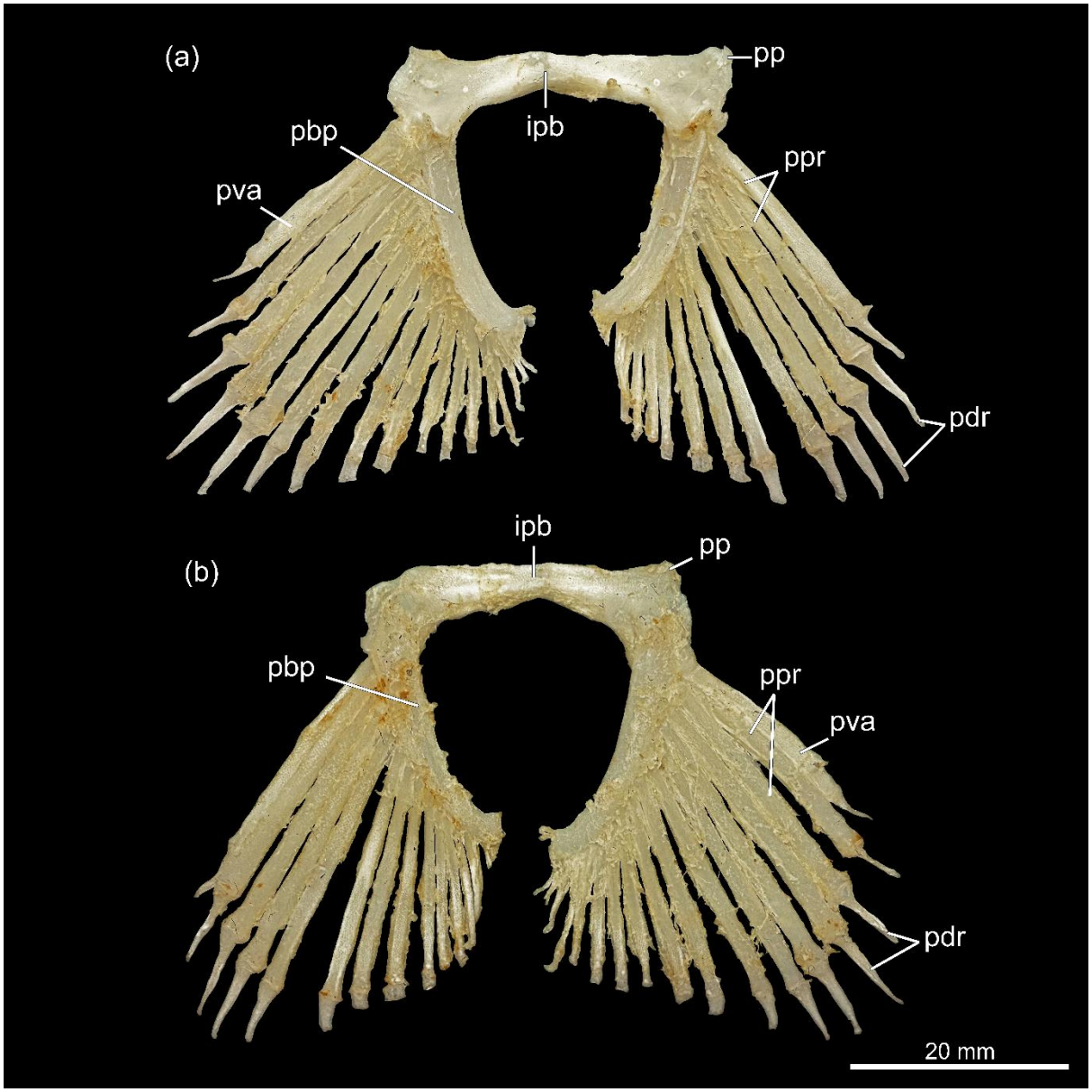


**Figure 17.** *Hemiscyllium ocellatum*, subadult female (EMRG-Chond-H-2): Different views of pelvic girdle. (a) dorsal and (b) ventral view. Abbreviations: ipb, puboischiatic bar; pbp, pelvic basipterygium; pdr, pelvic distal radial; pp, prepelvic process; ppr, pelvic proximal radial; pva, anterior pelvic basal cartilage.

#### *4.1.2.10 Vertebral column*

While head and fins were relatively easy to clean, the connective tissue surrounding the spine was sticking very strong to the cartilage. For this reason, only part of the vertebral column was exposed to avoid damage. The genus *Hemiscyllium* usually has 180 to 195 vertebrae (Ebert et al. 2021), while the count for *Hemiscyllium ocellatum* on average ranges from 183 to 197 centra (Allen et al. 2016). The amphicoelous centrum is of cylindrical shape and can be divided into the notochordal sheath complex and the calcified layers (Goto 2001). The vertebral centra show the typical asterospondyl calcification pattern of Orectolobiformes, giving it a star-like appearance (Figure 18c). Vertebrae can be divided into abdominal vertebrae, anterior of the cloaca, precaudal vertebrae, between cloaca and caudal fin and caudal vertebrae forming the dorsal lobe of the caudal fin (Goto 2001). The major differences between these three, apart from size, is the presence of a haemal arch, positioned ventrally, carrying the caudal artery and vein, and the division in monospondylous and diplospondylous vertebrae. The absence of a haemal arch can be observed in the abdominal vertebrae, while it is incomplete in the precaudal vertebrae and present in the caudal vertebrae(Figure 18a,b,c) (Goto 2001). The distinction between monospondylous and diplospondylous vertebrae exclusively applies within abdominal and precaudal vertebrae. In monospondylous vertebrae, which are characterised by the presence of ribs, each body segment is associated with a single vertebra. Conversely, the diplospondylous vertebrae, which do not bear ribs, exhibit a different anatomical configuration, with two vertebrae present within a single body segment (Goto 2001).

The neural arch of the vertebral column is lightly connected to the connective tissue, making it challenging to uncover it. According to Goto (2001),

the neural arch in orectolobiforms consists of a basidorsal process, a dorsal intercalary plate and a supraneural. Together they from the neural canal containing the spinal cord and blood vessels (Figure 18a,b,c).

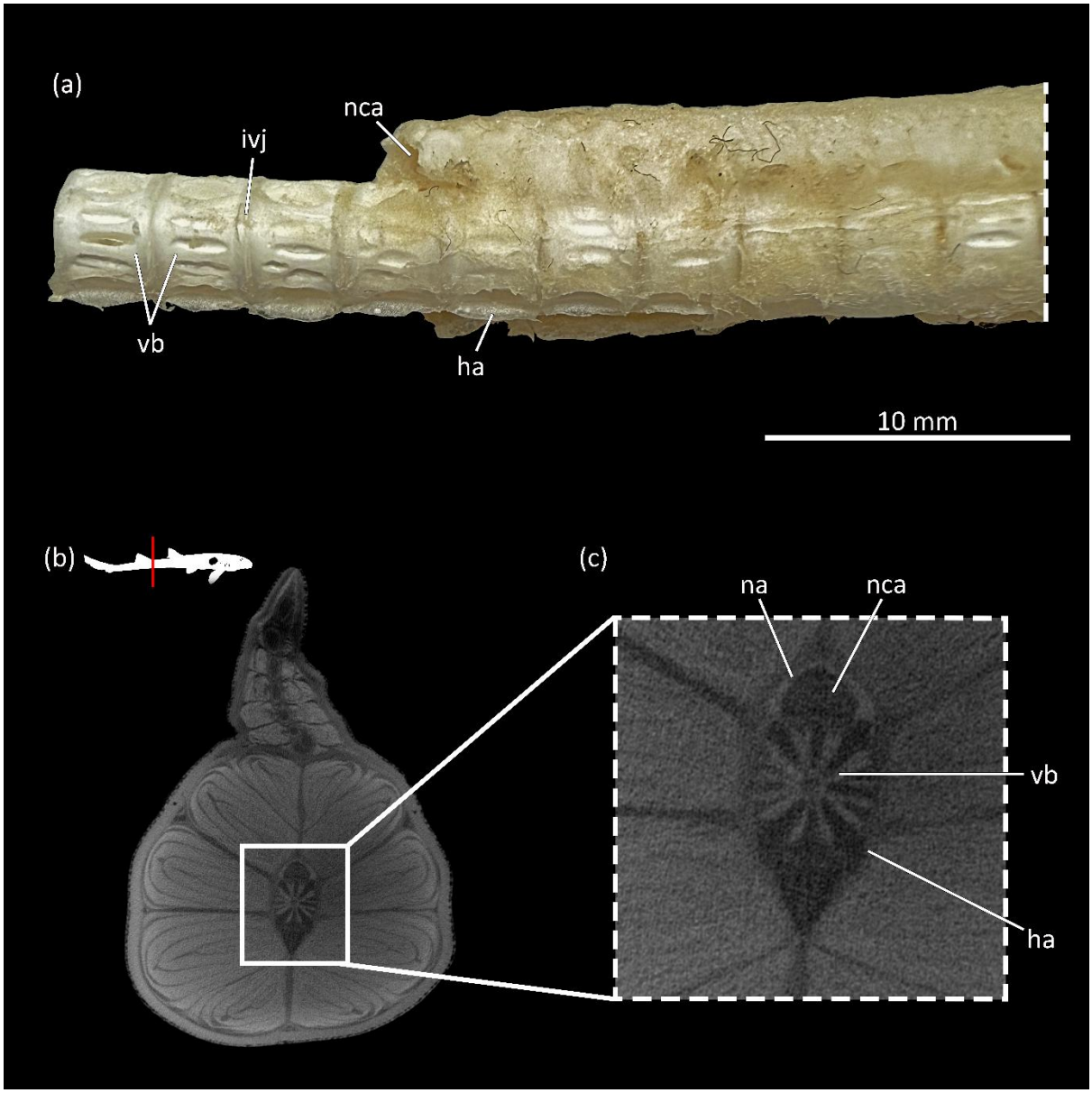


**Figure 18.** *Hemiscyllium ocellatum*, top subadult female (EMRG-Chond-H-2), bottom male (EMRG-Chond-A-5): Dissected vertebral column and Ct scan of the first dorsal fin region. (a) lateral view, (b) CT scan overview and (c) detail of vertebral column in CT scan. Abbreviations: nca, neural canal; ivj, intervertebral joint; vb, vertebral body; ha, haemal arch; na, neural arch.

## 4.2 Discussion

### 4.2.1 Methodological discussion

The study combines traditional anatomical methods (dissection) with modern imaging techniques (micro-CT). Each method has its own merits, which, when combined, have the potential to provide new insights into morphological aspects in vertebrates.

The successful staining of the dorsal fin sections of a male specimen of *Hemiscyllium ocellatum* with iodine, according to the method of Degenhardt et al. (2010), allows for non-destructive, high-resolution micro-CT imaging of the analysed structures, which includes various soft and hard tissues. Highly calcified skeletal elements such as cartilage and soft tissues, like muscles, and connective tissue can be differentiated with high contrast. The long time required for the staining process is necessary for visualizing these structures effectively. These results align with previous applications of iodine-enhanced micro-CT approach in elasmobranch studies (Staggl et al. 2022; 2023) and show its advantages over non-stained micro-CT imaging.

The dissection of the female specimen allows for direct insight into the musculoskeletal system of *H. ocellatum*, which might not be discernible with micro-CT scans. It enables a detailed examination of the individual muscles, cartilages, and their articulations. This facilitates the identification of subtle structures, like the multilayered composition of several muscles, such as the *musculi inclinatores dorsales*, which might not be entirely possible with micro-CT imaging alone (Staggl et al. 2022). Another positive aspect is the incomparable insight into skeletal articulations, the texture of muscles, and the orientation of individual muscle fibres. However, due to high adhesion of skin and connective tissue, especially in the fin regions, certain structures were difficult to expose without damage, and some unfortunately even got severely damaged, which is why they were not visible in situ.

A comparison of the two methods for visualising morphological structures demonstrates that this integrative approach offers a unique insight into the (internal) morphology of an organism. Dissection, however, is limited in some respects as for example the fragility of some tissues and the destruction of the specimen, which allows only a single application. To minimise errors, it is therefore advisable to work on one side only, so that potentially damaged structures can be worked out more carefully on the second side. In contrast, micro-CT imaging enables repeated scanning without damaging the specimen, thus

allowing its preservation for future analyses. This enables others to verify the results themselves or to carry out further studies on the organism, although more preparation time is needed, and the general effort is higher due to several preceding steps (e.g. staining). In addition, some fine structures, particularly those with low iodine absorption (e.g. uncalcified connective tissue) were still hardly visible. The combination of both approaches allows a more complete understanding and interpretation of the functional anatomy, which minimizes the potential loss of essential information.

### 4.2.2 Morphological discussion

Epaulette sharks are commonly encountered in shallow waters, lagoons and tidal pools of coral reefs (Ebert et al. 2021). Coral reefs are complex, three-dimensional habitats providing a variety of overhangs, tunnels and crevices (Graham & Nash 2013). This not only supports high species richness (Chabanet et al. 1997; Graham & Nash 2013; Risk 1972), but also a high variety of types of locomotion (Schakmann & Korsmeyer 2023; Sims 2010). Epaulette sharks, like most representatives of the family Hemiscyllidae (bamboo sharks), are well adapted to this habitat. Their slender, elongated body and versatile fins allow them to manoeuvre efficiently through the heterogenous coral reef environment. Hemiscyllids characteristically dwell in close proximity to the ground and typically exhibit a gaited movement that can be described as a combination of walking and trotting (Goto et al. 1999; Pridmore 1994).

As part of the anatomical examination, several morphological features were identified, that are not only relevant for locomotion, but also for feeding mechanisms and general lifestyle of *H. ocellatum*. Detailed structures could be described in the head region, the dorsal, and the paired fins, like the double layered *musculi inclinatores dorsales* and the strongly pronounced muscles in the pectoral and pelvic fins. In comparison to other orectolobiforms, *H. ocellatum* (Goto 2001; Shirai 1992) shows further advanced adaptations to a benthic lifestyle.

The head region and especially the mouth region shows typical traits of a benthic suction feeder. From the slightly dorsoventrally flattened head to the subterminal orientated mouth opening. The most prominent muscles which are important for the generation of the suction force are hypobranchial muscles, especially the *musculus coraco-branchialis* and the *musculus rectus cervicis* consisting of the *musculus coraco-arcualis* and the *musculus coraco-hyoideus* (Motta et al. 2008).

The segmented muscle groups of the dorsal fins, the *musculi inclinatores dorsales*, were described for the first time for *H. ocellatum*. Aligning with the observations made by Medeiros et al. (2024) in *C. punctatum*, they are layered muscles, tightly packed around the dorsal fin radials, and the distal part of the dorsal fin basals. With them originating from the basals and inserting into the radials they are likely to aid a precise control of the dorsal fins. The addition of micro-CT scans to the methods used by Medeiros et al. (2024) clearly showed the fine dividing line between the two parts of the dorsal inclinator muscles, which was hard to see during the dissection.

The investigation of the skeleton of the pectoral and pelvic girdles, as well as the associated muscles, confirm the findings of (Goto et al. 1999), and provide potential new functional intimations. The paired fins seemingly facilitate a high degree of mobility and control, which is required for benthic locomotion. Extended basal elements, robust articulations, and highly developed depressor and levator muscles mentioned by Goto et al. (1999) in coordination with the higher rotational potential of the pectoral and pelvic girdle described by Pridmore (1994) support the previously mentioned walking-trot. Morphological dissections of the pectoral and pelvic fins emphasise this specialisation of the paired fins to enable this type of “walking” similar to terrestrial locomotion. In the pectoral fins, the multilayered levator muscles (*musculus levator pectoralis superficialis*, *inferior*, and *distalis*) together with the elongated basal cartilages (meso- and metapterygium) seem to increase leverage across multiple axes. The strongly developed *musculus depressor pectoralis* pushes the pectoral fin against the substrate and consequently pulls the body forward. The pelvic fins show a different organizational pattern. Again, a levator and depressor muscle can be identified, but unlike the pectoral fin muscles, they appear to be single layered. The *musculus levator pelvicus* covers the dorsal surface of the fin and connects to the *musculus hypaxialis* on the lateral body wall, which potentially enables a higher pulling force. The *musculus depressor pelvicus* is positioned more anteriorly and distally as in the pectoral fin and is supplemented by an *musculus adductor pelvicus*, allowing for finer control of rotational fin movements. The combination of elongated basal cartilages (anterior basal cartilage and basipterygium) and connection of the *musculus levator pelvicus* to the lateral body wall further increases leverage across multiple axes. The specific subdivisions of the depressor pelvicus and the presence of the adductor pelvicus in addition to a better control of fin

movements, possibly increases the strength to lift the body from the ground and push it forward.

## 4.3 Conclusion

This study aimed to give a detailed morphological description of the musculoskeletal system of *H. ocellatum*. By using a combination of manual dissection and micro-CT imaging, the study provides a detailed description of the pectoral and pelvic gridle, cranial structures, the unpaired fins, and the associated musculature. The primary objective was to examine how skeletal and muscular structures contribute to the special walking-like locomotion and suction feeding behaviour of *H. ocellatum*. The results confirmed the assumption that *H. ocellatum* possesses specific morphological adaptations for a walking motion in the pectoral and pelvic girdle. The muscles seem to aid in high mobility of the fins and efficient benthic locomotion. This supports the first hypothesis and shows the basis of the terrestrial-like locomotion.

The combination of traditional and digital anatomical methods allowed for a comprehensive description of both, surface-level and deep structures and provided meaningful addition to previous studies. It also enabled the identification of structures (e.g. separation of the two layers of *musculi inclinatores dorsales*) that were barely visible during the dissection, which again highlights the complementary nature of the methods.

Functionally and evolutionary the results could be significant in showing that these morphological modifications are adaptations to the requirements of the complex coral reef habitats und could represent evolutionary stepping stones toward more terrestrial-like modes of locomotion, serving as potential analogies to a fin-to-limb transition in early tetrapods.

Thus, the anatomic data produced in this study contribute valuable information to further comparative studies within the Orectolobiformes but also serve as a necessary foundation for the second part of this work.

# 5 Morphofunctional Walking and Suction Feeding

## 5.1 Results

During several recording sessions different movement patterns were observed (Figures 19, 20 and 21). The typical “crawling movement”, sometimes compared to that of salamanders and also observed in other studies (Goto et al. 1999; Pridmore 1994), was displayed several times (Figure 19a,b,c,d,e). As described by Pridmore (1994) and observed in neonate and juvenile individuals by Porter et al. (2022), three types of gaits were expressed by the specimen. In addition to the pectoral girdles’ and pelvic fins’ rotation that were described by Pridmore (1994), a contralateral folding of the dorsal fins was observed during the walking locomotion (Figures 19a,b,c,d,e and 20a,b,c,d,e). Furthermore, a special movement sequence seen during the suction feeding was observed during the recording period (Figure 21a,b,c,d,e).

### 5.1.1 Walking motion

The three gaits shown by the two specimens are (1) a swimming gait without contact to the substrate, (2) a fast-walking gait and (3) a slow walking gait. Due to the experimental setup, it was not possible to film the swimming gait, but the specimens moved as described by Pridmore (1994) and Porter et al. (2022), as undulating movement with lateral bending of the whole body.

The two walking gaits differ in step frequency and unwind as follows. A closer examination of the dorsal and pelvic and pectoral fins reveals a coordinated pattern of movement, i.e., the bending of the dorsal fins is closely linked to the rotation of the pectoral and especially the pelvic fins, and the resulting lateral bending of the body (Figure 19a,b,c,d,e). Specifically, when the left pelvic fin makes a forward movement, the body bends to the left, causing the first dorsal fin to lean in the same direction (Figure 19b,c). The second dorsal fin follows this motion shortly afterwards (Figure 20a,b,c). Finishing the rotation of the pelvic fins, the dorsal fins follow and return to a central, neutral position (Figure 19c). In the same way, a forward movement with the right pelvic fin leads to the first dorsal fin being leant left and shortly afterwards, the second dorsal fin follows the same direction (Figure 19d).

A comparison of the two dorsal fins reveals that the first dorsal fin always reacts first, with the second dorsal fin following within a second. Additionally, the tilting of the first dorsal fin appears to be more pronounced than the one from the second dorsal fin (Figure 20c,d). In an ongoing movement along the substrate, the pattern is as follows:

1. Left pectoral fin steps forward.
2. Left pectoral fin pulls the body forward along the substrate, while the left pelvic fin simultaneously steps forward (Figure 19d).
3. First dorsal fin folds to the left (Figure 19d).
4. Initially, the second dorsal fin stays neutral, but after a short time (within a second), it folds to the left in coordination with the first dorsal fin. During this phase, the body bends to the left (Figure 19e).
5. As the left pelvic fin pushes the body forward, the right pectoral fin steps forward and initiates the next pulling movement (Figure 19d).
6. The right pelvic fin advances, triggering a rightward fold of the first dorsal fin.
7. The two dorsal fins now temporarily fold in opposite directions (Figure 20b), until the second dorsal fin follows the first into a rightward fold (Figure 20c). This sequence results in a rightward bend of the body (Figures 19a and 20c).

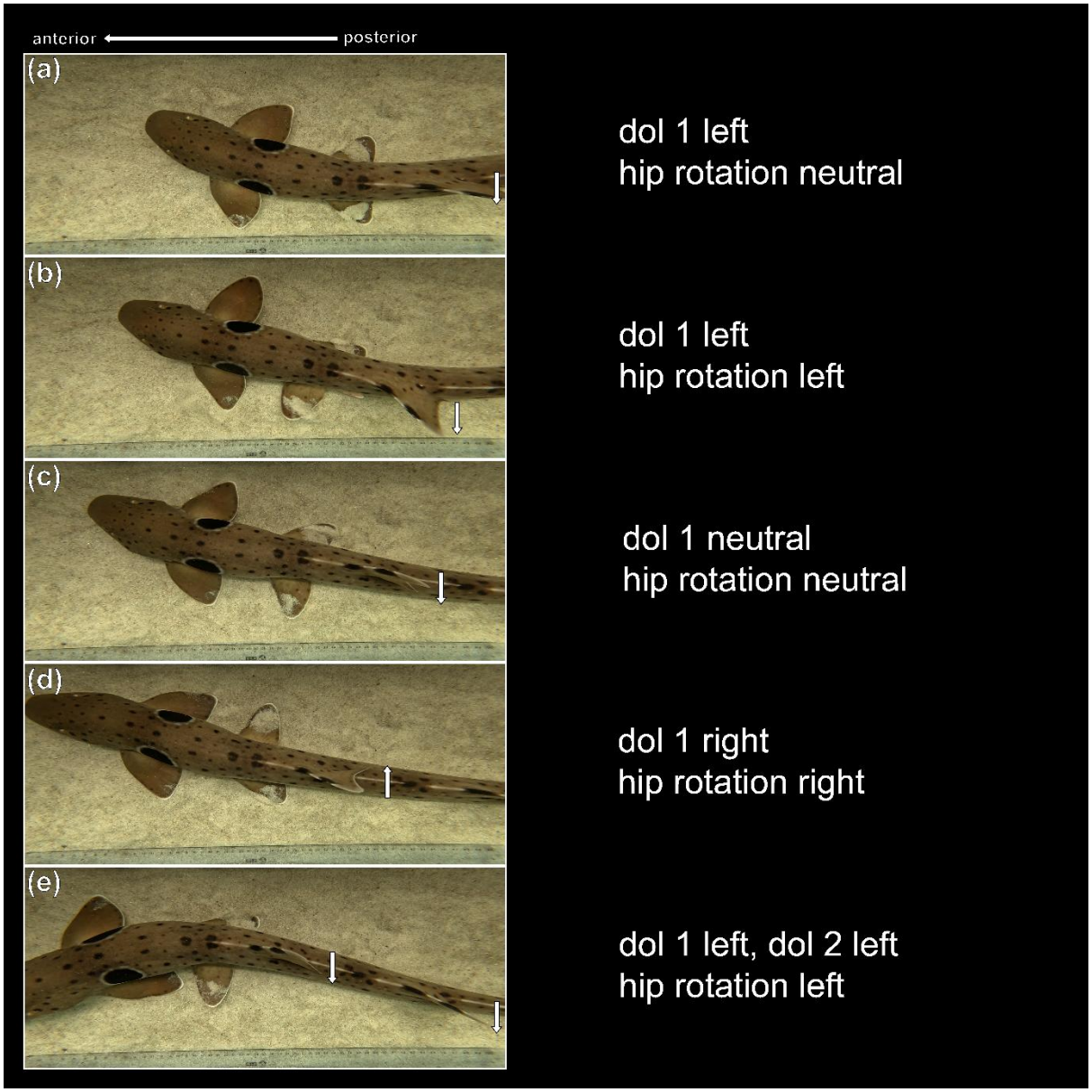


**Figure 19.** *Hemiscyllium ocellatum*, male: Dorsal view of sequence of pelvic and dorsal fin movement while walking on substrate. (a) right bend, (b) "step" with left pelvic fin, (c) forward motion, (d) "step" with right pelvic fin, and (e) left bend of body. Abbreviations: dol 1, first dorsal fin; dol 2, second dorsal fin.

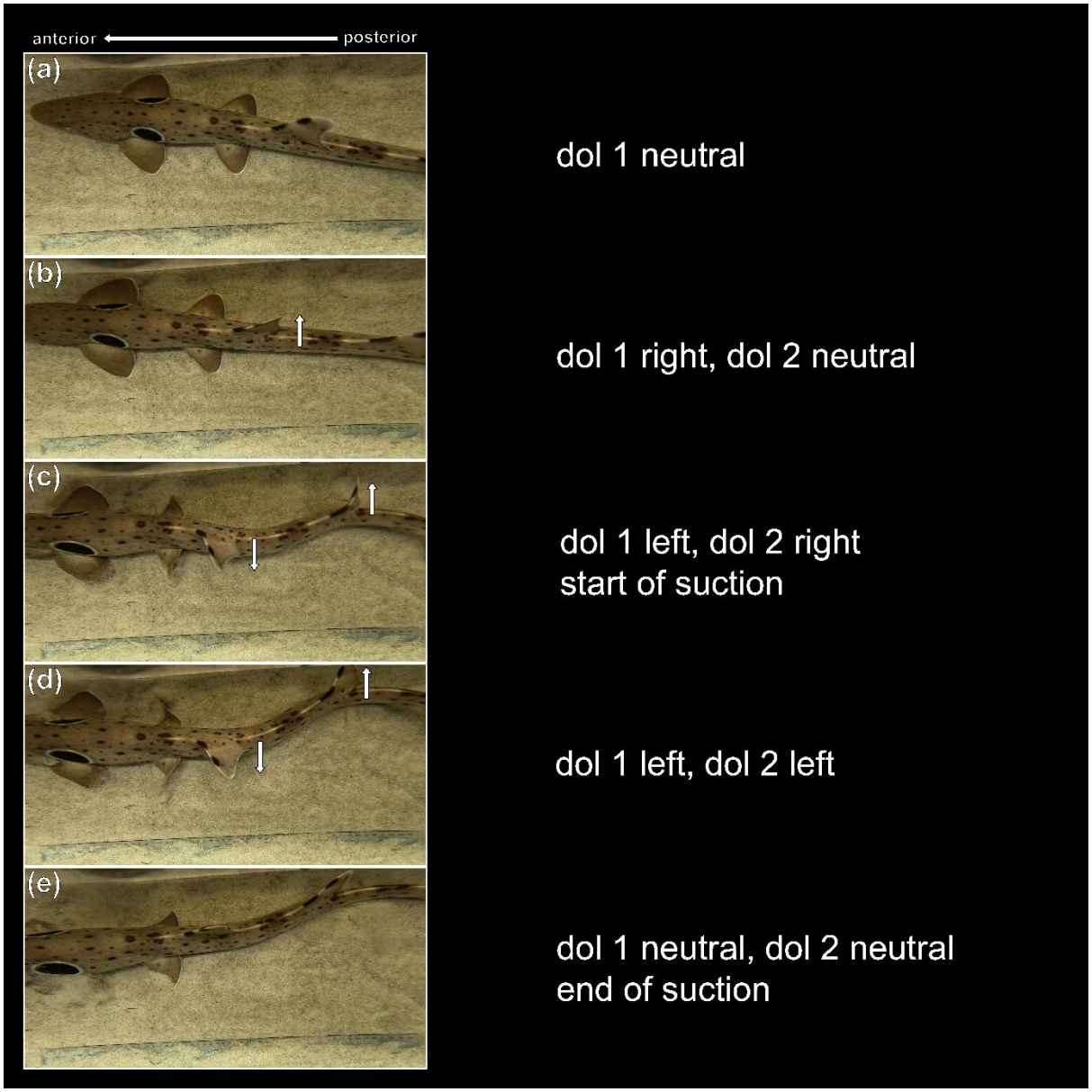


**Figure 20.** *Hemiscyllium ocellatum*, male: Dorsal view of sequence of dorsal fin movement while walking on substrate. (a) left bend, (b) beginning right bend, (c) right bend, (d) beginning left bend, and (e) left bend of body. Abbreviations: dol 1, first dorsal fin; dol 2, second dorsal fin.

### 5.1.2 Suction feeding

Another pattern noticed was a distinct movement during food intake. Here, the whole body of *Hemiscyllium ocellatum* seems to play a role. In addition to the previously described movement, which also was performed during movement towards a food source, a different, hitherto unrecognized movement pattern of pectoral, pelvic and dorsal fins is used. During the feeding process, the typical suction procedure was observed in combination with a sigmoidal curvature of the body and placing the fins against the current (Figure 21c,d). This mechanism unwinds as follows:

- Suction starts as mouth opens and simultaneously s-shaped bending of body.
- Posterior edges of pectoral and pelvic fins are raised, and dorsal fins strongly tilt into opposite directions (Figure 21c,d).

Both performances occur within a fraction of a second. At the same time as the food source is sucked in, the body relaxes, which results in neutral re-positioning of all fins and the straightening of the body (Figure 21e).

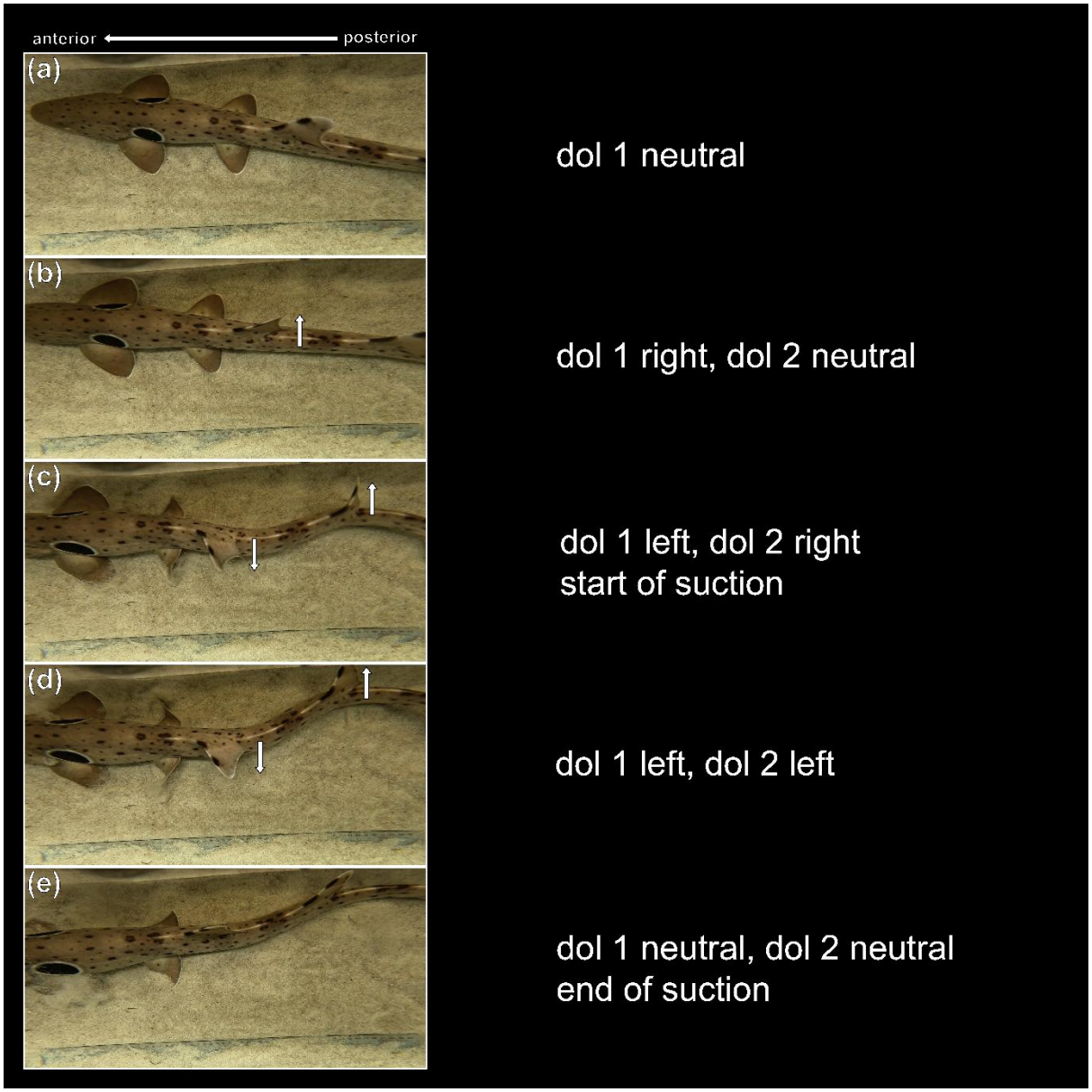


**Figure 21.** *Hemiscyllium ocellatum*, female: Dorsal view of movement pattern during suction feeding. (a) neutral body position, (b) movement towards food source, (c) start of suction, (d) intake of food source, and (e) end of suction and swallowing. Abbreviations: dol 1, first dorsal fin; dol 2, second dorsal fin;

## 5.2 Discussion

### 5.2.1 Methodological discussion

The study uses video recordings during feeding sessions to enable behavioural analysis while walking and suction feeding. The video recordings play a crucial role in putting the movement patterns in context to actions of the musculoskeletal system. It enables to record multiple locomotion sequences, allowing for the identification of different gaits, fin-, and movement coordination during suction feeding. Also, it was possible to describe the previously unknown coordinated movement of the dorsal fins in combination with the paired fins during "walking". This unique way of locomotion could not have been described with static anatomical models and data alone. Thus, video analysis serves as a link between the observation of locomotion patterns and the involvement of the respective musculature and skeletal elements. The only limitations encountered during the filming sessions were due to the controlled environment and the experimental layout. The water depth of the tank did not allow for detailed recordings of the whole specimen, which means that only the movement of certain parts of the body could be documented at once. Here, deeper depths of the aquarium or better camera equipment is necessary to take more complete recordings.

### 5.2.2 Morphofunctional discussion

Their way of hunting often requires *H. ocellatum* to walk, sometimes just slightly submerged, over exposed reef tops to get from one tidepool to the next one (Gervais et al. 2018; Routley et al. 2002). The ability of the epaulette shark to hunt in these areas is primarily based on the high hypoxia tolerance (Heinrich et al. 2014; Heinrich et al. 2016; Routley et al. 2002; Wise et al. 1998) and the special nature of their fins (Goto et al. 1999). A central observation in this study was the coordination of the pectoral, pelvic, and dorsal fins with body undulation during benthic locomotion. The video recordings confirmed the different types of gaits already mentioned in the study conducted by Porter et al. (2022), which is already observed in the neonatal stage: slow and fast walking-gait and swimming. The walking-gait is comparable to the locomotion of some tetrapods (Hildebrand 1966). The pronounced walking locomotion observed in *H. ocellatum* seems to be a defining synapomorphy of the genus (*Hemiscyllium*) (Allen et al. 2016), distinguishing it from other genera within the family Hemiscyllidae, which show it to a lesser extent or not at all. It is particularly suitable for structurally complex

environments, where manoeuvring through narrow spaces is essential for foraging and habitat utilization (Gillis 1998; Pridmore 1994). This enables *H. ocellatum* to exploit ecological niches inaccessible to more pelagic or less agile benthic taxa (Dudgeon et al. 2020; Heupel & Bennett 1998).

New insights were gained into the functional role of the dorsal fins during locomotion. Both dorsal fins were observed to incline laterally in coordination with the undulating body and paired fins movements. Bending of the body seems to initiate inclination of the first dorsal fin in the opposite direction of the bend, followed right after by the second dorsal fin. In a study by Maia and Wilga (2013), the muscle activity of the dorsal fins of *C. punctatum* (Hemiscyllidae) and *Squalus acanthias* (Squalidae) was compared, thereby providing evidence that the dorsal fins play an active role in locomotion. In *C. punctatum* the dorsal fins seem to actively aid in the later stages of a turn, enabling tighter turnings. The close relationship and the similar habitat could suggest similar functions in *H. ocellatum*. Since *C. punctatum* is less specialized for walking locomotion (Goto et al. 1999), other functions in *H. ocellatum* cannot be ruled out. The specific inclination of the dorsal fins suggests a potential stabilisation or resistance-reducing function. It could also aid the body undulation and directional changes of movement, by helping to keep the body level and aligned during movement. Also, since an integration of dorsal fin activity into benthic locomotion has not been reported for other orectolobiform sharks, it may represent a derived feature within the genus *Hemiscyllium*. A potential basis for the folding of the dorsal fins could be the *musculi inclinatores dorsales*, which have been examined in different species, including the closely related *C. punctatum* by Medeiros et al. (2024) morphologically. But despite the similar composition in *C. punctatum* (Medeiros et al. 2024), the unique dorsal fin movement has, for now, just been observed in *H. ocellatum*. Still, the *musculi inclinatores dorsales* could be a potential explanation for the special type of contra-lateral fin inclination during locomotion and suction feeding.

Furthermore, results obtained revealed a particular movement pattern during suction feeding. The powerful suction force generated for the caption of prey pulls the sharks body forward, also visible in the conducted video recordings. As seen in the videos, *H. ocellatum* adjusts body posture during suction feeding and fin alignment to increase its surface area facing the direction of movement. This helps to counteract the forward pull caused by the suction, as the larger surface area creates more resistance against the water. The resulting

drag slows the shark's forward motion, potentially making the suction more effective for drawing prey in.

## 5.3 Conclusion

Building upon the anatomical foundation established in previous works, this study focused on the behavioural and morphofunctional aspects of *H. ocellatum*. It aimed to give new insights into the well-known benthic walking behaviour with a focus on the paired and dorsal fins, as well as their involvement during suction feeding. For the first time, the contralateral inclination of the dorsal fins during benthic locomotion and suction feeding could be documented. It revealed a coordinated, alternating fin movement pattern also involving both of the paired fins.

A novel observation during this study was the specific positioning of the body and fins to seemingly counteract the force of the suction during feeding. Such a function has been underappreciated functional studies of elasmobranchs to date and could indicate a broader involvement in locomotion than assumed, especially of the dorsal fins.

These findings support the second hypothesis, assuming an active function of the dorsal fins during walking and suction feeding.

From a methodological standpoint, the video analysis in combination with anatomical data shows great potential for functional interpretations of locomotion patterns. It enabled a detailed insight into the synergy of morphology and behaviour. Nevertheless, certain limitations must be acknowledged, like the limited sample size for video recordings and challenges in interpreting some video sequences due to field of view restraints. This however opens the door to further studies to refine the methodology.

Given the paucity of literature concerning the walking behaviour and suction feeding pattern of different species, except for *H. ocellatum*, it is recommended that further investigations of these behaviours be conducted not only in the epaulette shark, but also in other members of the Orectolobiformes.

# 6 Acknowledgments

First and foremost, I would like to express my sincere gratitude to my supervisor, Prof. Dr. **Jürgen Kriwet**, for the invaluable guidance, and expertise provided throughout the course of this thesis and the chance to write it at the EvoMoRG. Your mentorship has been a cornerstone of this project and my academic growth.

I also wish to thank my co-supervisor, **Manuel Andreas Staggl**, MSc., for your insightful feedback, support, and constructive discussions, which have greatly enriched the quality of this work. Without your constant availability and willingness to help I would not have been able to finish my master thesis in the given time. I would particularly like to emphasize the many hours in which you taught me various techniques, whether on the computer or with the scalpel.

A special thank you goes to **Frederik Mollen**, whose generous support in providing the two *Hemiscyllium ocellatum* specimens enabled both the dissections and micro-CT scans. This thesis could not have been realized without your contribution.

I would also like to express my gratitude to Dr. **Cathrin Pfaff**, whose dedication and technical skills as head of the micro-CT lab for our working group made a significant contribution to this study.

To my colleagues and fellow students - thank you for the stimulating conversations, constructive feedback, and supportive environment throughout these past semesters. Working and learning alongside you has been a rewarding experience.

I am deeply grateful to my family for their unwavering support, patience, and encouragement during this journey. Your financial support and belief in me, as well as the curiosity and determination you have given me on my way helped me persevere through every step of the process.

Lastly, to my friends and especially **Raphaela Jernej** - thank you for your love, understanding, and continuous support. Your presence and exemplary effect have been a source of strength and balance, and I am immensely grateful for your companionship during this intense and transformative time.

# 7 References

**Allen, G. R., Erdmann, M. V., White, W. T., Fahmi, & Dudgeon, C. L.** (2016). Review Of The Bamboo Shark Genus Hemiscyllium (Orectolobiformes: Hemiscyllidae). Advance online publication. https://doi.org/10.5281/zenodo.164197

**Andreev, P. S., Coates, M. I., Shelton, R. M., Cooper, P. R., Smith, M. P., & Sansom, I. J.** (2015). Upper Ordovician chondrichthyan-like scales from North America. *Palaeontology*, *58*(4), 691–704. https://doi.org/10.1111/pala.12167

**Baum, J. K., & Worm, B.** (2009). Cascading top-down effects of changing oceanic predator abundances. *The Journal of Animal Ecology*, *78*(4), 699–714. https://doi.org/10.1111/j.1365-2656.2009.01531.x

**Brazeau, M. D., & Friedman, M.** (2015). The origin and early phylogenetic history of jawed vertebrates. *Nature*, *520*(7548), 490–497. https://doi.org/10.1038/nature14438

**Burrow, C. J., Turner, S., Trinajstic, K., & Young, G. C.** (2019). Late Silurian vertebrate microfossils from the Carnarvon Basin, Western Australia. *Alcheringa: An Australasian Journal of Palaeontology*, *43*(2), 204–219. https://doi.org/10.1080/03115518.2019.1566496

**Carrier, J. C., Simpfendorfer, C. A., Heithaus, M. R., & Yopak, K. E.** (Eds.). (2022). *Biology of Sharks and Their Relatives*. CRC Press. https://doi.org/10.1201/9781003262190

**Chabanet, P., Ralambondrainy, H., Amanieu, M., Faure, G., & Galzin, R.** (1997). Relationships between coral reef substrata and fish. *Coral Reefs*, *16*(2), 93–102. https://doi.org/10.1007/s003380050063

**Compagno, L. J. V., Didier, D. A., & Burgess, G. H.** (2005). Classification of Chondrichthyan Fish. In S. L. Fowler (Ed.), *Sharks, rays and chimaeras: The status of the chondrichthyan fishes: status survey* (pp. 4–11). IUCN - The World Conservation Union; available from IUCN Publications Services Unit.

**Cortes, E.** (1999). Standardized diet compositions and trophic levels of sharks. *ICES Journal of Marine Science*, *56*(5), 707–717. https://doi.org/10.1006/jmsc.1999.0489

**De Iuliis, G.** (2011). *The Dissection of Vertebrates* (2nd ed.). Elsevier Science & Technology. https://ebookcentral.proquest.com/lib/kxp/detail.action?docID=7270459

**Degenhardt, K., Wright, A. C., Horng, D., Padmanabhan, A., & Epstein, J. A.** (2010). Rapid 3D phenotyping of cardiovascular development in mouse embryos by micro-CT with

iodine staining. *Circulation. Cardiovascular Imaging*, *3*(3), 314–322. https://doi.org/10.1161/CIRCIMAGING.109.918482

**Denton, J. S. S., Maisey, J. G., Grace, M., Pradel, A., Doosey, M. H., Bart, H. L., & Naylor, G. J. P.** (2018). Cranial morphology in Mollisquama sp. (Squaliformes; Dalatiidae) and patterns of cranial evolution in dalatiid sharks. *Journal of Anatomy*, *233*(1), 15–32. https://doi.org/10.1111/joa.12823

**Dudgeon, C. L., Corrigan, S., Yang, L., Allen, G. R., Erdmann, M. V., Fahmi, Sugeha, H. Y., White, W. T., & Naylor, G. J. P.** (2020). Walking, swimming or hitching a ride? Phylogenetics and biogeography of the walking shark genus Hemiscyllium. *Marine and Freshwater Research*, *71*(9), 1107. https://doi.org/10.1071/MF19163

**Ebert, Dando, M., & Fowler, S. L.** (2021). *Sharks of the world: A complete guide*. Princeton University Press. https://www.degruyter.com/document/isbn/9780691210872/html https://doi.org/10.1515/9780691210872

**Elizondo-Omaña, R. E., Guzmán-López, S., & García-Rodríguez, M. D. L. A.** (2005). Dissection as a teaching tool: Past, present, and future. *Anatomical Record. Part B, New Anatomist*, *285*(1), 11–15. https://doi.org/10.1002/ar.b.20070

**Feitosa, L. M., & Nunes, J. L. S.** (2020). New Record of Carcharhinus leucas in an Amazonian river system. *Boletim Do Laboratório De Hidrobiologia*, *30*(1). https://doi.org/10.18764/1981-6421e2020.6

**Flammang, B. E.** (2010). Functional morphology of the radialis muscle in shark tails. *Journal of Morphology*, *271*(3), 340–352. https://doi.org/10.1002/jmor.10801

**Frazzetta, T. H.** (1994). Feeding Mechanisms in Sharks and Other Elasmobranchs. In R. G. Liège, V. L. Bels, M. Chardon, & P. Vandewalle (Eds.), *Advances in Comparative and Environmental Physiology. Biomechanics of Feeding in Vertebrates* (Vol. 18, pp. 31–57). Springer Berlin Heidelberg. https://doi.org/10.1007/978-3-642-57906-6_3

**Fricke, R., Eschmeyer, W. N., & van der Laan, R.** (2025). *Eschmeyer's Catalog of Fishes: Genera, Species, References*. http://researcharchive.calacademy.org/research/ichthyology/catalog/fishcatmain.asp

**Gauthier, A. R. G., Whitehead, D. L., Tibbetts, I. R., & Bennett, M. B.** (2019). Comparative morphology of the electrosensory system of the epaulette shark Hemiscyllium

ocellatum and brown-banded bamboo shark Chiloscyllium punctatum. *Journal of Fish Biology*, *94*(2), 313–319. https://doi.org/10.1111/jfb.13893

**Gervais, C. R., Nay, T. J., Renshaw, G., Johansen, J. L., Steffensen, J. F., & Rummer, J. L.** (2018). Too hot to handle? Using movement to alleviate effects of elevated temperatures in a benthic elasmobranch, Hemiscyllium ocellatum. *Marine Biology*, *165*(11). https://doi.org/10.1007/s00227-018-3427-7

**Gignac, P. M., Kley, N. J., Clarke, J. A., Colbert, M. W., Morhardt, A. C., Cerio, D., Cost, I. N., Cox, P. G., Daza, J. D., Early, C. M., Echols, M. S., Henkelman, R. M., Herdina, A. N., Holliday, C. M., Li, Z., Mahlow, K., Merchant, S., Müller, J., Orsbon, C. P., . . . Witmer, L. M.** (2016). Diffusible iodine-based contrast-enhanced computed tomography (diceCT): An emerging tool for rapid, high-resolution, 3-D imaging of metazoan soft tissues. *Journal of Anatomy*, *228*(6), 889–909. https://doi.org/10.1111/joa.12449

**Gillis, G. B.** (1998). Environmental Effects on Undulatory Locomotion in the American Eel Anguilla Rostrata: Kinematics in Water and on Land. *Journal of Experimental Biology*, *201*(7), 949–961. https://doi.org/10.1242/jeb.201.7.949

**Goldschmid, A.** (2014). Chondrichthyes, Knorpelfische. In W. Westheide & G. Rieger (Eds.), *Spezielle Zoologie. Teil 2: Wirbel- oder Schädeltiere* (3. Aufl. 2015, pp. 202–224). Springer Berlin Heidelberg. http://nbn-resolving.org/urn:nbn:de:bsz:31-epflicht-1548101

**Goto, T.** (2001). Comparative Anatomy, Phylogeny and Cladistic Classification of the Order Orectolobiformes (Chondrichthyes, Elasmobranchii). *Memoirs of the Graduate School of Fisheries Sciences, Hokkaido University*(48(1)), 1–100. http://hdl.handle.net/2115/22014

**Goto, T., Nishida, K., & Nakaya, K.** (1999). Internal morphology and function of paired fins in the epaulette shark,hemiscyllium ocellatum. *Ichthyological Research*, *46*(3), 281–287. https://doi.org/10.1007/BF02678514

**Graham, N. A. J., & Nash, K. L.** (2013). The importance of structural complexity in coral reef ecosystems. *Coral Reefs*, *32*(2), 315–326. https://doi.org/10.1007/s00338-012-0984-y

**Grogan, E., & Lund, R.** (2004). The Origin and Relationships of Early Chondrichthyes. In J. A. Musick, J. C. Carrier, & M. R. Heithaus (Eds.), *Marine Biology. Biology of Sharks and*

*Their Relatives* (Vol. 20043354, pp. 3–31). CRC Press. https://doi.org/10.1201/9780203491317.pt1

**Grogan, E., Lund, R., & Greenfest-Allen, E.** (2012). The Origin and Relationships of Early Chondrichthyans. In J. C. Carrier, J. A. Musick, & M. R. Heithaus (Eds.), *CRC Marine Biology Ser. Biology of Sharks and Their Relatives, Second Edition* (2nd ed., Vol. 20123460, pp. 3–29). Taylor and Francis. https://doi.org/10.1201/b11867-3

**Hammerschlag, N., Herskowitz, Y., Fallows, C., & Couto, T. B. A.** (2025). Evidence of cascading ecosystem effects following the loss of white sharks from False Bay, South Africa. *Frontiers in Marine Science*, *12*, Article 1530362. https://doi.org/10.3389/fmars.2025.1530362

**Heinrich, D. D. U., Rummer, J. L., Morash, A. J., Watson, S.-A., Simpfendorfer, C. A., Heupel, M. R., & Munday, P. L.** (2014). A product of its environment: The epaulette shark (Hemiscyllium ocellatum) exhibits physiological tolerance to elevated environmental CO2. *Conservation Physiology*, *2*(1), cou047. https://doi.org/10.1093/conphys/cou047

**Heinrich, D. D. U., Watson, S.-A., Rummer, J. L., Brandl, S. J., Simpfendorfer, C. A., Heupel, M. R., & Munday, P. L.** (2016). Foraging behaviour of the epaulette shark Hemiscyllium ocellatum is not affected by elevated CO2. *ICES Journal of Marine Science*, *73*(3), 633–640. https://doi.org/10.1093/icesjms/fsv085

**Heupel, M. R., & Bennett, M. B.** (1998). Observations on the diet and feeding habits of the epaulette shark, Hemiscyllium ocellatum (Bonnaterre), on Heron Island Reef, Great Barrier Reef, Australia. *Marine and Freshwater Research*, *49*(7), 753. https://doi.org/10.1071/MF97026

**Heupel, M. R., Whittier, J. M., & Bennett, M. B.** (1999). Plasma steroid hormone profiles and reproductive biology of the epaulette shark,Hemiscyllium ocellatum. *The Journal of Experimental Zoology*, *284*(5), 586–594. https://doi.org/10.1002/(SICI)1097-010X(19991001)284:5<586::AID-JEZ14>3.0.CO;2-B

**Hildebrand, M.** (1966). Analysis of the symmetrical gait sof tetrapods. *Folia Biotheoretica*(6), 9–22.

**Holmgren, N.** (1940). Studies on the Head in Fishes: Embryological, Morphological, and Phylogenetical Researches. *Acta Zoologica*, *21*(1-3), 51–266. https://doi.org/10.1111/j.1463-6395.1940.tb00339.x

**Jabado, R., Morata, A., Bennett, R., Finucci, B., Ellis, J., Fowler, S., Grant, M., Barbosa Martins, A., & Sinclair, S.** (2024). *The global status of sharks, rays, and chimaeras.* IUCN Species Survival Commission Shark Specialist Group. https://doi.org/10.59216/ssg.gsrsrc.2024

K**eklikoglou, K., Arvanitidis, C., Chatzigeorgiou, G., Chatzinikolaou, E., Karagiannidis, E., Koletsa, T., Magoulas, A., Makris, K., Mavrothalassitis, G., Papanagnou, E.-D., Papazoglou, A. S., Pavloudi, C., Trougakos, I. P., Vasileiadou, K., & Vogiatzi, A.** (2021). Micro-CT for Biological and Biomedical Studies: A Comparison of Imaging Techniques. *Journal of Imaging*, *7*(9). https://doi.org/10.3390/jimaging7090172

**Klimpfinger, C., & Kriwet, J.** (2020). Comparative morphology of labial cartilages in sharks (Chondrichthyes, Elasmobranchii). *The European Zoological Journal*, *87*(1), 741–753. https://doi.org/10.1080/24750263.2020.1844323

**Last, P. R. R., & Stevens, J. D. D.** (Eds.). (1994). *Sharks and Rays of Australia*. CSIRO Publishing.

**Maia, A., & Wilga, C. D.** (2013). Anatomy and muscle activity of the dorsal fins in bamboo sharks and spiny dogfish during turning maneuvers. *Journal of Morphology*, *274*(11), 1288–1298. https://doi.org/10.1002/jmor.20179

**Maisey, J. G.** (1996). *Discovering fossil fishes* (1. ed.). *A Peter N. Nevraumont book*. Holt.

**Maisey, J. G., Denton, J. S. S., Burrow, C., & Pradel, A.** (2021). Architectural and ultrastructural features of tessellated calcified cartilage in modern and extinct chondrichthyan fishes. *Journal of Fish Biology*, *98*(4), 919–941. https://doi.org/10.1111/jfb.14376

**Mallatt, J.** (1996). Ventilation and the origin of jawed vertebrates: a new mouth. *Zoological Journal of the Linnean Society*, *117*(4), 329–404. https://doi.org/10.1006/zjls.1996.0043

**Medeiros, J., Vaz, D. F. B., Araújo, M. V. G., Lima, A. de, & Da Silva, J. P. C. B.** (2024). Morphology and phylogenetic implications of the inclinatores dorsales for the galeomorph sharks (Chondrichthyes: Elasmobranchii). *Journal of Anatomy.* Advance online publication. https://doi.org/10.1111/joa.14162

**Metscher, B. D.** (2009). Microct for comparative morphology: Simple staining methods allow high-contrast 3D imaging of diverse non-mineralized animal tissues. *BMC Physiology*, *9*, 11. https://doi.org/10.1186/1472-6793-9-11

**Miyake, T., & McEachran, J. D.** (1991). The morphology and evolution of the ventral gill arch skeleton in batoid fishes (Chondrichthyes: Batoidea). *Zoological Journal of the Linnean Society*, *102*(1), 75–100. https://doi.org/10.1111/j.1096-3642.1991.tb01537.x

**Motta, P. J., Hueter, R. E., Tricas, T. C., Summers, A. P., Huber, D. R., Lowry, D., Mara, K. R., Matott, M. P., Whitenack, L. B., & Wintzer, A. P.** (2008). Functional morphology of the feeding apparatus, feeding constraints, and suction performance in the nurse shark Ginglymostoma cirratum. *Journal of Morphology*, *269*(9), 1041–1055. https://doi.org/10.1002/jmor.10626

**Motta, P. J., & Wilga, C. D.** (2001). Advances in the Study of Feeding Behaviors, Mechanisms, and Mechanics of Sharks. *Environmental Biology of Fishes*, *60*(1-3), 131–156. https://doi.org/10.1023/A:1007649900712

**Musick, J. A., & Ellis, J. K.** (2005). Reproductive Evolution of Chondrichthyans. In W. C. Hamlett (Ed.), *Reproductive Biology and Phylogeny of Chondrichthyes: Sharks, Batoids and Chimaeras* (pp. 45–79). CRC Press.

**Nay, T. J., Longbottom, R. J., Gervais, C. R., Johansen, J. L., Steffensen, J. F., Rummer, J. L., & Hoey, A. S.** (2021). Regulate or tolerate: Thermal strategy of a coral reef flat resident, the epaulette shark, Hemiscyllium ocellatum. *Journal of Fish Biology*, *98*(3), 723–732. https://doi.org/10.1111/jfb.14616

**Nelson, J. S., Grande, T. C., & Wilson, M. V. H.** (2016). *Fishes of the World*. Wiley. https://doi.org/10.1002/9781119174844

**Porter, M. E., Hernandez, A. V., Gervais, C. R., & Rummer, J. L.** (2022). Aquatic Walking and Swimming Kinematics of Neonate and Juvenile Epaulette Sharks. *Integrative and Comparative Biology*, *62*(6), 1710–1724. https://doi.org/10.1093/icb/icac127

**Pridmore, P. A.** (1994). Submerged walking in the epaulette shark Hemiscyllium ocellatum (Hemiscyllidae) and its implications for locomotion in rhipidistian fishes and early tetrapods. *Zoology*, 278–297. https://cir.nii.ac.jp/crid/1572543024951077120

**Renshaw, G. M. C., Kerrisk, C. B., & Nilsson, G. E.** (2002). The role of adenosine in the anoxic survival of the epaulette shark, Hemiscyllium ocellatum. *Comparative Biochemistry and Physiology. Part B, Biochemistry & Molecular Biology*, *131*(2), 133–141. https://doi.org/10.1016/S1096-4959(01)00484-5

**Risk, M. J.** (1972). Fish Diversity on a Coral Reef in the Virgin Islands. *Atoll Research Bulletin*, *153*, 1–4. https://doi.org/10.5479/si.00775630.153.1

**Routley, M. H., Nilsson, G. E., & Renshaw, G. M. C.** (2002). Exposure to hypoxia primes the respiratory and metabolic responses of the epaulette shark to progressive hypoxia. *Comparative Biochemistry and Physiology. Part A, Molecular & Integrative Physiology*, *131*(2), 313–321. https://doi.org/10.1016/S1095-6433(01)00484-6

**Rowat, D., & Brooks, K. S.** (2012). A review of the biology, fisheries and conservation of the whale shark Rhincodon typus. *Journal of Fish Biology*, *80*(5), 1019–1056. https://doi.org/10.1111/j.1095-8649.2012.03252.x

**Schakmann, M., & Korsmeyer, K. E.** (2023). Fish swimming mode and body morphology affect the energetics of swimming in a wave-surge water flow. *Journal of Experimental Biology*, *226*(6). https://doi.org/10.1242/jeb.244739

**Schilling, T., & Thorogood, P.** (2000). Development and evolutionof the vertebrate skull. In P. O'Higgins (Ed.), *Linnean Society symposium series: Vol. 20. Development, growth and evolution: Implications for the study of the hominid skeleton* (Vol. 20, pp. 57–83). Academic Press.

**Shirai, S.** (1992). Squalean Phylogeny: a New Framework of " Squaloid " Sharks and Related Taxa. *Hokkaido University Press*, *1992*, 151 pp.

**Sims, D. W.** (2010). Swimming Behaviour and Energetics of Free-ranging Sharks: New Directions in Movement Analysis. In P. Domenici & B. G. Kapoor (Eds.), *Fish Locomotion* (pp. 407–435). CRC Press. https://doi.org/10.1201/b10190-13

**Soares, M. C., & Carvalho, M. R. de** (2013). Mandibular and hyoid muscles of Galeomorph sharks (Chondrichthyes: Elasmobranchii), with remarks on their phylogenetic intrarelationships. *Journal of Morphology*, *274*(10), 1111–1123. https://doi.org/10.1002/jmor.20166

**Staggl, M. A., Abed-Navandi, D., & Kriwet, J.** (2022). Cranial morphology of the orectolobiform shark, Chiloscyllium punctatum Müller & Henle, 1838. *Vertebrate Zoology*, *72*, 311–370. https://doi.org/10.3897/vz.72.e84732

**Staggl, M. A., Ruthensteiner, B., & Straube, N.** (2023). Head anatomy of a lantern shark wet-collection specimen (Chondrichthyes: Etmopteridae). *Journal of Anatomy*, *242*(5), 872–890. https://doi.org/10.1111/joa.13822

**Weigmann, S.** (2016). Annotated checklist of the living sharks, batoids and chimaeras (Chondrichthyes) of the world, with a focus on biogeographical diversity. *Journal of Fish Biology*, *88*(3), 837–1037. https://doi.org/10.1111/jfb.12874

**White, W. T., O'Neill, H. L., & Naylor, G. J. P.** (2022). Taxonomy and Diversity of Extant Elasmobranchs. In J. C. Carrier, C. A. Simpfendorfer, M. R. Heithaus, & K. E. Yopak (Eds.), *Biology of Sharks and Their Relatives* (pp. 31–57). CRC Press.

**Whitenack, L. B., Kim, S. L., & Sibert, E. C.** (2022). Bridging the Gap Between Chondrichthyan Paleobiology and Biology. In J. C. Carrier, C. A. Simpfendorfer, M. R. Heithaus, & K. E. Yopak (Eds.), *Biology of Sharks and Their Relatives* (pp. 1–29). CRC Press.

**Wilga, C. D.** (2005). Morphology and evolution of the jaw suspension in lamniform sharks. *Journal of Morphology*, *265*(1), 102–119. https://doi.org/10.1002/jmor.10342

**Wilga, C. D., & Sanford, C. P.** (2008). Suction generation in white-spotted bamboo sharks Chiloscyllium plagiosum. *The Journal of Experimental Biology*, *211*(Pt 19), 3128–3138. https://doi.org/10.1242/jeb.018002

**Winther-Janson, M., Wueringer, B. E., & Seymour, J. E.** (2012). Electroreceptive and mechanoreceptive anatomical specialisations in the epaulette shark (Hemiscyllium ocellatum). *PloS One*, *7*(11), e49857. https://doi.org/10.1371/journal.pone.0049857

**Wise, G., Mulvey, J. M., & Renshaw, G. M. C.** (1998). Hypoxia tolerance in the epaulette shark (Hemiscyllium ocellatum). *The Journal of Experimental Zoology*, *281*(1), 1–5. https://doi.org/10.1002/(SICI)1097-010X(19980501)281:1<1::AID-JEZ1>3.0.CO;2-S